

1 Hydrogen isotope fractionation in leaf waxes in the Alaskan Arctic tundra

2

3 William C. Daniels^{1,2*}, James M. Russell¹, Anne E. Giblin², Jeffrey M. Welker³, Eric S.
4 Klein³, Yongsong Huang^{1*}

5

6 1. Brown University, Department of Earth, Environment, and Planetary Sciences, 324
7 Brook St., Providence, RI, 02906.

8 2. Marine Biological Laboratory, The Ecosystems Center, 7 MBL St., Woods Hole, MA,
9 02543

10 3. University of Alaska-Anchorage, Department of Biological Sciences, 3211 Providence
11 Dr., Anchorage, AK 99508

12 Email addresses: william_daniels@brown.edu, james_russell@brown.edu,
13 agiblin@mbl.edu, jmwelker@uaa.alaska.edu, esklein@uaa.alaska.edu,
14 yongsong_huang@brown.edu

15 *Corresponding authors

16

17 Abstract

18 Leaf wax hydrogen isotopes (δD_{wax}) are increasingly utilized in terrestrial
19 paleoclimate research. Applications of this proxy must be grounded by studies of the
20 modern controls on δD_{wax} , including the ecophysiological controls on isotope
21 fractionation at both the plant and landscape scales. Several calibration studies suggest a
22 considerably smaller apparent fractionation between source water and waxes (ϵ_{app}) at
23 high latitudes relative to temperate or tropical locations, with major implications for
24 paleoclimatic interpretations of sedimentary δD_{wax} . Here we investigate apparent
25 fractionation in the Arctic by tracing the isotopic composition of leaf waxes from
26 production in modern plants to deposition in lake sediments using isotopic observations
27 of precipitation, soil and plant waters, living leaf waxes, and waxes in sediment traps in
28 the Brooks Range foothills of northern Alaska. We also analyze a lake surface sediment
29 transect to compare present-day vegetation assemblages to ϵ_{app} at the watershed scale.
30 Source water and ϵ_{app} were determined for live specimens of *Eriophorum vaginatum*
31 (cottongrass) and *Betula nana* (dwarf birch), two dominant tundra plants in the Brooks
32 Range foothills. The δD of these plants' xylem water closely tracks that of surface soil
33 water, and reflects a summer-biased precipitation source. Leaf water is enriched by $23 \pm$
34 15‰ relative to xylem water for *E. vaginatum* and by $41 \pm 19\text{‰}$ for *B. nana*.
35 Evapotranspiration modeling indicates that this leaf water enrichment is consistent with
36 the evaporative enrichment expected under the climate conditions of northern Alaska, and
37 that 24-hour photosynthesis does not cause excessive leaf water isotope enrichment. The
38 ϵ_{app} determined for our study species average $-89 \pm 14\text{‰}$ and $-106 \pm 16\text{‰}$ for *B. nana n*-
39 alkanes and *n*-acids, respectively, and $-182 \pm 10\text{‰}$ and $-154 \pm 26\text{‰}$ for *E. vaginatum n*-

40 alkanes and *n*-acids, which are similar to the ϵ_{app} of related species in temperate and
41 tropical regions, indicating that apparent fractionation is similar in Arctic relative to other
42 regions, and there is no reduced fractionation in the Arctic. Sediment trap data suggest
43 that waxes are primarily transported into lakes from local (watershed-scale) sources by
44 overland flow during the spring freshet, and so δD_{wax} within lakes depends on watershed-
45 scale differences in water isotope compositions and in plant ecophysiology. As such, the
46 large difference between our study species suggests that the relative abundance of
47 graminoids and shrubs is potentially an important control on δD_{wax} in lake sediments.
48 These inferences are supported by δD_{wax} data from surface sediments of 24 lakes where
49 ϵ_{app} , relative to δD_{xylem} , averages $-128 \pm 13\text{‰}$ and $-130 \pm 8\text{‰}$ for *n*-acids and *n*-alkanes,
50 respectively, and co-varies with vegetation type across watersheds. These new
51 determinations of plant source water seasonality and ϵ_{app} for the Arctic will improve the
52 δD_{wax} paleoclimate proxy at high latitudes.

53

54 Keywords: Leaf waxes, Water isotopes, Biomarkers, Precipitation, Isotope fractionation,
55 Arctic, Tundra, Sediment

56

57 Highlights

- 58 • δD of source water for Arctic plants reflects a mixture of seasonal precipitation
59 dominated by summer rainfall.
- 60 • Net apparent fractionation between precipitation and leaf waxes in Arctic plants is
61 similar to that of temperate regions.

- 62 • Leaf waxes from *Eriophorum vaginatum*, a C₃ graminoid, are 23 - 76‰ more
63 depleted than *Betula nana*, a C₃ shrub.
- 64 • Lake sediment waxes are derived primarily from within watersheds, and ϵ_{app} in
65 lake sediments correlates with watershed-scale vegetation assemblages.

66

67 1. Introduction

68 Hydrogen and oxygen isotope ratios in meteoric water (δD and $\delta^{18}O$) are well-
69 established tracers of environmental processes (Dansgaard, 1964; Ehleringer and
70 Dawson, 1992; Vachon et al., 2010; Welker, 2012). When preserved in the geologic
71 record, these isotopes serve as robust tools for paleoclimate reconstructions (Feakins et
72 al., 2012; Jasechko et al., 2015; Klein et al., 2016; Konecky et al., 2016). Hydrogen
73 isotope ratios of plant leaf waxes are an increasingly utilized proxy because they are
74 abundant in many sediments (Huang et al., 2004; Sachse et al., 2004), are stable over
75 long time periods (Yang and Huang, 2003), and their isotopic composition (δD_{wax})
76 primarily reflects the δD of precipitation ($\delta D_{precipitation}$) (Sternberg, 1988; Sauer et al.,
77 2001; Huang et al., 2004; Sachse et al., 2004; Sachse et al., 2010). The δD_{wax} is depleted
78 by a fractionation factor (ϵ_{app}) relative to $\delta D_{precipitation}$ due to several isotope-
79 discriminating processes that occur between precipitation and leaf wax synthesis and
80 deposition (Sessions et al., 1999; Chikaraishi et al., 2004; Sachse et al., 2012; Kahmen et
81 al., 2013b). Accurate estimates of ϵ_{app} are therefore fundamentally important to guide
82 climatic interpretations of ancient δD_{wax} (Polissar and Freeman, 2010; Yang et al., 2011;
83 Garcin et al., 2012; Feakins, 2013; Niedermeyer et al., 2016), and ideally, to
84 quantitatively determine $\delta D_{precipitation}$ and climate variations in geological time.

85 Numerous analyses of δD_{wax} from lake sediments and living plants in temperate
86 and tropical regions have begun to converge on average ϵ_{app} values of -100 to -130‰
87 (Sauer et al., 2001; Sachse et al., 2004; Smith and Freeman, 2006; Hou et al., 2008;
88 Garcin et al., 2012; Kahmen et al., 2013a; Liu et al., 2016), with *n*-alkanes displaying
89 slightly greater isotope discrimination than *n*-alkanoic acids (Chikaraishi and Naraoka,
90 2007). Recent estimates of ϵ_{app} at high-latitude sites, however, are dramatically different.
91 Shanahan et al. (2013) estimated ϵ_{app} of -61‰ for C₂₆ and C₂₈ alkanolic-acids using lake
92 surface sediment samples from Baffin Island in the High Arctic (latitude: 63 to 73 °N)
93 compared against mean annual precipitation isotopes compositions for source water
94 estimated from the Online Isotopes in Precipitation Calculator (OIPC) geospatial model
95 (Bowen and Revenaugh, 2003). Porter et al. (2016) produced similar ϵ_{app} values for both
96 long-chain *n*-acids and long-chain *n*-alkanes by comparing fossil waxes to adjacent fossil
97 water (interpreted as mean annual precipitation formed simultaneously with the waxes) in
98 loess sections in the Canadian sub-Arctic (latitude: 63.5 °N). Based on growth chamber
99 experiments, these low ϵ_{app} values in high-latitude, continuous light environments have
100 been suggested to result from plant stomata remaining open throughout the 24-hour sunlit
101 period, thus driving high daily rates of evapotranspiration and high leaf water isotope
102 enrichment (Yang et al., 2009).

103 In contrast, Wilkie et al. (2012) studied lake sediment waxes (*n*-acids) in northern
104 Siberia (latitude: 67°N) and reported ϵ_{app} of -101‰ with respect to estimates of mean
105 annual precipitation isotope composition, and ϵ_{app} of -110‰ with respect to the measured
106 isotopic composition of spring streamflow. Sachse et al. (2004) report ϵ_{app} of -100 to -
107 135‰ for long chain *n*-alkanes from Arctic Europe using similar methods. These

108 contrasting results raise the following questions: 1) is ϵ_{app} latitude-dependent? 2) is ϵ_{app}
109 highly variable across high latitude biomes? and 3) are observations of small ϵ_{app} an
110 artifact of relying on estimated, rather than measured, source water isotope compositions?

111 The apparent fractionation of Arctic δD_{wax} is extremely important to
112 understanding past and current polar climate change. δD_{wax} records in polar regions have
113 been interpreted as both summer and mean annual temperature change on time-scales
114 from the Holocene to the Paleocene (Pagani et al., 2006; Feakins et al., 2012; Thomas et
115 al., 2012; Pautler et al., 2014; Porter et al., 2016), with implications for the Earth's
116 equilibrium climate sensitivity and future response to rising greenhouse gases. For
117 example, calculations of Paleocene/Eocene $\delta D_{precipitation}$ from ancient wax δD and an ϵ_{app}
118 of -100‰ to -130‰ reveal extreme warmth and moisture convergence in the Arctic
119 during the Paleocene/Eocene thermal maximum (PETM) (Pagani et al., 2006). If a
120 smaller ϵ_{app} of -60‰ is used, however, the estimated $\delta D_{precipitation}$ during this time period
121 was similar to modern $\delta D_{precipitation}$, and not strongly enriched, casting doubt on our
122 understanding of Arctic climate during the PETM. Paleoclimate inferences for Antarctica
123 during the mid-Miocene (Feakins et al., 2012) are likewise sensitive to whether an ϵ_{app}
124 value of -100‰ or -60‰ is used to calculate $\delta D_{precipitation}$. Similarly, two temperature
125 anomaly estimates for the last glacial maximum in western Canada (Pautler et al., 2014;
126 Porter et al., 2016), which rely on the same δD_{wax} data but different values of ϵ_{app} , differ
127 by 14°C. Clearly, large deviations of ϵ_{app} , caused either by inaccurate assessment of plant
128 source water δD values, by enhanced leaf water isotope enrichment during 24-hour
129 transpiration, or by large changes in vegetation assemblages, would complicate
130 interpretations of polar δD_{wax} .

131 With the exception of the study by Wilkie et al. (2012), investigations of ϵ_{app} in
132 the Arctic have thus far relied on estimated $\delta D_{precipitation}$ values from the OIPC model
133 (Bowen and Revenaugh, 2003; Yang et al., 2011; Shanahan et al., 2013) or measurements
134 of relict (frozen) water in permafrost (Porter et al., 2016). Both of these methods could be
135 insufficient for determining ϵ_{app} considering the complexity of precipitation seasonality,
136 soil water dynamics, and plant water use dynamics (Alstad et al., 1999; Welker et al.,
137 2005; Young et al., In press). Moreover, previous efforts to quantify the effects of 24-
138 hour photosynthesis in greenhouse experiments used plants that do not currently grow in
139 the Arctic, such as *Metasequoia* (redwood), and the hypothesized increase in leaf water
140 isotopic values due to greater transpiration was not accompanied by leaf water isotopic
141 measurements (Yang et al., 2009). Direct measurements of plant xylem and leaf waters in
142 Arctic field conditions would provide a more robust estimate of plant source water
143 isotope values (Welker, 2000; Leffler and Welker, 2013). To our knowledge, no previous
144 study has traced Arctic D/H fractionation from precipitation to leaf wax production in
145 living plant tissues, changes in δD_{wax} through the growing season, nor variations in δD_{wax}
146 associated with native Arctic vegetation, ecosystem integration, and sedimentation.

147 Three ecophysiological controls are particularly important to estimating ϵ_{app} . First,
148 the seasonal fluctuations in $\delta D_{precipitation}$ relative to the timing of wax synthesis by plants
149 can lead to differences in source water isotope composition for different regions or plant
150 types (Alstad et al., 1999; Vachon et al., 2010). Accurate determination of seasonal
151 changes in plant source water is especially important in the Arctic, where $\delta D_{precipitation}$ can
152 change drastically through the year. Secondly, although the δD of xylem water (δD_{xylem})
153 generally reflects $\delta D_{precipitation}$ (White et al., 1985), the δD of leaf water (δD_{leaf}) is

154 sensitive to factors that govern leaf water evaporation including relative humidity
155 (Kahmen et al., 2013a; Tipple et al., 2015), species effects (leaf morphology, canopy
156 height, water use efficiency) (Sullivan and Welker, 2007), and possibly day length (Yang
157 et al., 2009). Again, quantifying enrichment in δD_{leaf} in the Arctic could test whether
158 strong apparent fractionation results from 24-hour photosynthesis. Third, biosynthetic
159 fractionation during leaf wax generation varies by plant type. Eudicots are typically
160 characterized by ϵ_{app} value of -156 to -85‰ while monocotyledons have a larger
161 fractionation ranging from -190 to -120‰ (Hou et al., 2007; Gao et al., 2014a; Liu et al.,
162 2016). Fractionation values of arctic plants tend to fall into these ranges (Wilkie et al.,
163 2012; Thomas et al., 2016), although there is also support fractionation values as small as
164 60‰ at the plant-scale in the Arctic (Yang et al., 2011). Biosynthetic fractionation has
165 generally been treated as a species-specific constant, but Newberry et al. (2015) indicate
166 that biosynthetic fractionation varies seasonally because of the greater contribution of H
167 atoms from stored carbohydrates during the period of leaf flush. Together, these effects
168 may help explain the discrepancies in high-latitude estimates of ϵ_{app} , and also suggest that
169 shifting vegetation communities can significantly alter values of ϵ_{app} .

170 The main objectives of this study are 1) to assess the importance of 24-hour
171 daylight on D/H fractionation by determining ϵ_{app} at the plant and landscape scales in the
172 Arctic tundra, and 2) to describe the environmental controls, especially vegetation
173 assemblages, on δD_{wax} . We report paired measurements of the δD of precipitation, soil
174 water, xylem water, leaf water, and leaf waxes of two dominant plant taxa from the
175 Alaskan Arctic that constrain the apparent fractionation in these Arctic plants. We use
176 sediment trap data to assess changes in δD_{wax} through the growing season, and a regional

177 survey of leaf waxes preserved in lake surface sediment to estimate ϵ_{app} and evaluate
178 whether local vegetation variations explain between-lake variation in ϵ_{app} . Together, these
179 results provide a comprehensive framework for interpreting δD_{wax} in the Arctic tundra
180 and illustrate the utility of combining plant-level and ecosystem-level studies of D/H
181 fractionation.

182

183 2. Sites, samples, and methods

184

185 2.1 Site description

186 The study area is located in the northern foothills of the Brooks Range at the
187 Toolik Lake Natural Research Area (68.5 °N, 149.5 °W; Fig. 1). Annual temperature
188 averages -8.5 °C, while the summer (JJA) averages 9°C. Monthly temperatures are above
189 zero from mid-May to early-September. Precipitation averages 312 mm, with roughly
190 60% of precipitation occurring primarily as rain during summer months (JJA; Fig. 2)
191 (Cherry et al., 2014). Summer relative humidity averages 75%. The soils are
192 characterized by continuous permafrost with summer thaw depths ranging from 30 to 200
193 cm (Shaver et al., 2014). The growing season is characterized by an average date for first
194 leaf appearance of June 3, with full spring green-up occurring in late-June and plant
195 senescence occurring in late August and September (Toolik Environmental Data Center
196 Team, 2016).

197 Glacier activity emanating from the Brooks Range was spatially and temporally
198 variable through the late Pleistocene, giving rise to three landscape surfaces of varying
199 age and vegetation in our study area (Fig. 1) (Walker and Walker, 1996; Hamilton, 2003).

200 These consist of the Sagavanirktok (>125 ka), Itkillik I (~60 ka), and the Itkillik II (~25 –
201 11.5 ka) surfaces. The Sagavanirktok surface is gently sloping, has substantial organic
202 soil accumulations, and contains few lakes. The most recently deglaciated terrain (Itkillik
203 II) in contrast, has steeper slopes, shallow bedrock, and contains a higher density of
204 lakes; the Itkillik I surface is intermediate with regards to geomorphology. Vegetation
205 distributions across our study region are presented by Walker and Maier (2008), who
206 identify nine major vegetation classes. Of these, moist acidic tundra (MAT) is the most
207 prevalent and occurs on all landscapes (Fig. 1). MAT consists of tussock-sedges
208 (*Eriophorum vaginatum*), non-tussock sedges (*Carex bigelowii*), mosses, and dwarf
209 shrubs (primarily *Betula nana*). The younger glacial surfaces, being better drained, more
210 poorly weathered, and having shallower organic soils, tend to contain greater areas of dry
211 tundra complex and non-acidic tundra dominated by prostrate shrubs (*Salix arctic*, *S.*
212 *reticulata*) with a general absence of mosses and sedges, although MAT can also be
213 found on the younger surface. *Salix* and *Betula* complexes are commonly found along
214 streams and in watertracks. In general, similar plant communities can be found around
215 much of the Arctic (CAVM Team, 2003).

216

217 2.2 Sample collection

218

219 2.2.1 Vegetation and water isotopes

220 Precipitation isotopes were collected on a year-round event basis from 1993 to
221 present (Klein et al., 2016). Not all events were measured, but in total, the isotopic
222 composition of 254 precipitation events were measured. We calculated an amount-

223 weighted mean annual precipitation isotope signature using binned monthly values of
224 $\delta D_{\text{precipitation}}$ and monthly values of precipitation amount (Toolik LTER Environmental
225 Data Center).

226 Soil water and vegetation samples were collected on August 6, 2013, July 7/8,
227 2014, and August 7/8, 2014 between 10:00 and 16:00. Sampling sites were located within
228 the Imnavait Creek watershed (68.61 °N, 149.30 °W) on the Sagavanirktok glacial
229 surface and the Toolik Lake watershed (68.62 °N, 149.61 °W) on the Itkillik I glacial
230 surface. Both sites are characterized as moist acidic tundra, the most prevalent vegetation
231 community in the region. Soil water isotope profiles (δD_{soil}) were collected during each
232 sampling. Soil water was collected to a depth of 92.5 cm using two methods. We used
233 soil probes fit with a 50 mL syringe to extract water from the thawed organic horizon at
234 0, 5, 10, 15, and 20 cm soil depth. Water was pushed through a combusted GFF filter into
235 plastic scintillation vials and frozen. Where soil was too dry or frozen to use this method
236 we collected 5-10 cm³ soil samples from pits to be melted or distilled. Permafrost soil
237 samples were provided from soil pits dug by Colin Ward, Jason Dubkowski, and
238 Katherine Harrold of the ARC LTER (Ward and Cory, 2015).

239 We measured the δD_{xylem} , $\delta D_{\text{leaf water}}$, and δD_{wax} for two tundra plants, *Eriophorum*
240 *vaginatum* (cottongrass) and *Betula nana* (dwarf birch). These species are two of the
241 most dominant species in the Arctic tundra (Walker et al., 1994; Chapin III et al., 1995)
242 and serve as model species for monocots (*E. vaginatum*) and dicots (*B. nana*), which are
243 two major plant groupings with respect to D/H fractionation (Gao et al., 2014a). From the
244 same sites where soil water was collected, sets of roots, stems, and leaves from individual
245 plants were collected. A total of 14 sets of *B. nana* and 9 sets of *E. vaginatum* samples

246 were collected across all sampling efforts. Live roots were separated from aboveground
247 components and immediately cleaned of clinging soil and soil water. For *B. nana*, several
248 5-cm segments of stem were cut from each plant and composited. Likewise, >20 *B. nana*
249 leaves were collected and composited to ensure sufficient leaf water yield for isotopic
250 analyses and to homogenize variability among leaves. For *E. vaginatum*, stems were not
251 distinguished from leaves, and approximately 20 leaves were composited for each plant.
252 All plant parts were stored frozen in Whirlpak™ bags until processing.

253

254 2.2.2 Sedimentary waxes

255 We analyzed δD_{wax} from surface sediment samples from 24 lakes near Toolik
256 Field Station to compare to our ϵ_{app} values from individual plants and to assess the
257 ecosystem-integrated values of ϵ_{app} (Fig. 1). Lakes were selected that are accessible by
258 foot and that span the various glacial surfaces and vegetation types (Table 2). Surface
259 sediments were collected from lake depocenters in 2011 and 2013 using a gravity corer,
260 sectioned in the field, and kept frozen until analysis (Longo et al., 2016). We analyzed
261 the surface 1.0 cm from all lakes, which based on ^{210}Pb -based accumulation rates from
262 Lakes E5, Fog2, Upper Capsule, and Toolik, integrates 10-25 years (Daniels, unpublished
263 data). To test if local (watershed-scale) differences in vegetation assemblages can affect
264 the ϵ_{app} observed in lake sediments, we compared the ϵ_{app} with the relative abundance of
265 major vegetation types within each lake's watershed using single and multiple linear
266 regression. Vegetation distributions were derived from vegetation maps, which translate
267 aerial photographs into nine discrete plant complexes, downloaded from the Alaska
268 Geobotany Center (Walker and Maier, 2008)(Fig. 1, Table 2).

269 Sediments were also collected from sediment traps deployed in Toolik Lake and
270 Lake E5 (ARC LTER). Sediment traps were deployed in May 2014 and collection vials
271 were replaced 4 times during the summer giving 2-6 week resolution. Traps were
272 deployed approximately 2 m above the lake floor.

273

274 2.3. Sample processing and analysis

275

276 2.3.1 Water isotopes

277 Water was extracted from plant tissues and bulk soils using cryogenic vacuum
278 distillation (Gao et al., 2012). Soil and plant samples were heated under vacuum in
279 extraction vials to 100 °C and the resulting vapor was collected in a vial in liquid
280 nitrogen. Samples were immediately thawed and transferred into 4 mL vials, sealed with
281 parafilm, and stored at 4 °C. For all soil water samples, 3 mg of activated charcoal
282 (particle size <150 µm) was added to the samples to remove excessive dissolved organic
283 matter. Samples reacted overnight and the charcoal was filtered using a GFF filter.
284 Precipitation, soil water, and plant water samples were analyzed for $\delta^{18}\text{O}$ and δD on a
285 Picarro L1102-i cavity ring-down spectrometer at Brown University. Samples were
286 analyzed with Picarro ChemCorrect software to test for the effects of organic
287 contaminants and no samples were flagged as problematic. The 1σ analytical error
288 determined from replicate standards was 0.09‰ for $\delta^{18}\text{O}$ and 0.57‰ for δD .

289

290 2.3.2 Biomarker processing

291 Lipids were extracted from leaf residues after removing leaf water.
292 Approximately 100 mg of leaf material was sonicated for 15 minutes in
293 dichloromethane:methanol (1:1 v/v), with three solvent rinses. Lipids were extracted
294 from freeze-dried surface sediments and sediment trap samples using a Dionex
295 Accelerated Solvent Extractor (ASE) 350 with dichloromethane:methanol (9:1 v/v).
296 Lipids were separated following the methods of Gao et al. (2011). The total lipid extract
297 (TLE) was split into a acid and neutral fractions using aminopropyl silica gel
298 chromatography with dichloromethane:Isopropanol and 5% glacial acetic acid in ether as
299 eluents. An internal standard (7 μg *cis*-eicosenoic acid) was then added to the acid
300 fraction. Acids were methylated overnight at 60 °C with acidified anhydrous methanol of
301 a known isotopic composition. δD values of individual *n*-acids were later corrected for
302 the isotopic contribution incurred during methylation. Aliphatic compounds were isolated
303 from the neutral fraction by silica gel chromatography with sequential elution by hexane
304 (N1), dichloromethane (N2), and methanol (N4). The N1 fraction was spiked with an
305 internal standard of hexamethylbenzene. A sample blank was analyzed with every batch.

306 The *n*-alkane and *n*-acid distributions of all samples were determined using
307 Agilent 6890 gas chromatograph with a flame ionization detector (GC-FID). Compound-
308 specific isotope ratios ($\delta\text{D}_{\text{wax}}$) of long chain ($\text{C}_{22}\text{-C}_{31}$) molecules were measured on a
309 Thermo Finnigan Delta +XL isotope ratio mass spectrometer with a HP 6890 gas
310 chromatograph and a high-temperature pyrolysis reactor for sample introduction. For
311 both GC-FID and GC-IRMS analyses, the GC was fit with a 30 m HP1-MS column and
312 the heating protocol was as follows: injector was set to pulsed splitless mode at 320 °C;
313 the oven temperature was held at 70 °C for 1 minutes, then ramped by 25 °C min^{-1} to 230

314 °C, then by 6°C min⁻¹ to 315 °C minutes. The pyrolysis reactor temperature was set to
 315 1445 °C and the flow rate was held constant at 1.4 ml min⁻¹. The H3+ factor was
 316 determined every other day and averaged 2.7 (1σ = 0.3) during the course of analyses.
 317 Each sample was measured once on GC-FID and at least twice on GC-IRMS. Isotopic
 318 values were accepted if the voltage response was between 2 and 6 volts. A standard
 319 mixture containing either C₁₆, C₁₈, C₂₂, C₂₆, and C₂₈ *n*-acids or C₂₅, C₂₇, C₂₉, C₃₀, and C₃₂
 320 *n*-alkanes was analyzed between every six injections to monitor instrument accuracy, and
 321 corrections were made on daily batches for offsets between measured and reported
 322 standard values. Analytical uncertainty was calculated using the pooled standard
 323 deviation (Eq. 1). The 1σ uncertainties are reported in Table A1 and are consistently
 324 smaller than 3%.

325 Eq. 1: $\sigma = \sqrt{\frac{\sum(n_i-1)*s_i^2}{\sum(n_i-1)}}$, where i=day for standards and i=sample for samples.

326

327 2.3.3 Notation and Statistics

328 The carbon preference index (CPI), a metric of wax degradation and
 329 contamination (Bray and Evans, 1961), is calculated using Equations 2 and 3, while
 330 average change length (ACL) data is calculated using Equation 4.

331 Eq. 2: $CPI_{n-acids} = \frac{2*\sum_{i=20}^{30} i*C_i (i=evens)}{\sum_{i=19}^{29} i*C_i + \sum_{i=21}^{31} i*C_i (i=odds)}$, where i is the carbon number and

332 C is the concentration;

333 Eq. 3: $CPI_{n-alkanes} = \frac{2*\sum_{i=23}^{33} i*C_i (i=odds)}{\sum_{i=22}^{32} i*C_i + \sum_{i=24}^{34} i*C_i (i=evens)}$

334 Eq. 4 $ACL = \frac{\sum_{20}^{33} i*C_i}{\sum_{20}^{33} C_i}$

335 The isotopic composition of water and waxes is described in delta-notation (Eq.
336 5). Hydrogen isotope enrichment factors, ϵ , were calculated between two reservoirs as in
337 Equation 6.

338 Eq. 5: δD (‰) = $\left(\frac{R_{sample}}{R_{standard}} - 1 \right) \times 1000$, where $R = \frac{D}{H}$, and the standard is
339 Vienna standard mean ocean water (VSMOW).

340 Eq. 6: $\epsilon_{A-B} = \left[\frac{\delta D_A + 1000}{\delta D_B + 1000} - 1 \right] * 1000$.

341

342 3. Results

343

344 3.1 Plant source water

345 The $\delta D_{precipitation}$ is most enriched during summer and most depleted during winter
346 (Fig. 2), with a precipitation-weighted mean annual value of -166‰ and a mean summer
347 value of -139‰. The mean annual $\delta D_{precipitation}$ determined by the Online Isotope in
348 Precipitation Calculator is -159‰ (Bowen and Revenaugh, 2003; Bowen, 2015), slightly
349 enriched relative to observations. OIPC modeled monthly values are also somewhat
350 enriched, with a RMSE of 32‰ relative to observations.

351 In July the surface (0-1 cm) δD_{soil} averages -161.5‰, not significantly different
352 than mean annual $\delta D_{precipitation}$ ($p=0.27$) whereas in August, surface δD_{soil} is more
353 enriched than annual $\delta D_{precipitation}$ with values averaging -142‰ ($p=0.0003$) (Fig. 3).
354 Vertical profiles in δD_{soil} also differ between months. In July, there is a shift at
355 intermediate (10-30 cm) depth to values more negative than the permafrost, possibly a
356 result of residual winter precipitation. In contrast, in August there is a steady D-depletion

357 with depth. Permafrost δD_{soil} is assumed to be constant and has a value of -162 ± 6 , the
358 same as mean annual precipitation ($p=0.54$). Soil water isotopes fall on the local meteoric
359 water line (LMWL), indicating little effect of soil evaporation (Fig. 4). As such, the
360 progressive enrichment of surface soil water isotopes from July to August likely reflects
361 an increasing contribution of summer rains to the soil water pool.

362 Xylem water isotopes overlap with the LMWL and with soil water isotopes in
363 $\delta^{18}\text{O}$ - δD space (Fig. 4), indicating there is little to no fractionation during plant uptake,
364 consistent with previous studies (Ehleringer and Dawson, 1992). Overall, there is no
365 difference in δD_{xylem} between *E. vaginatum* and *B. nana* ($p = 0.084$). The δD_{xylem}
366 increases from -160 ± 8 to -147 ± 9 between July and August, tracking the enrichment in
367 δD_{soil} (Figure 5).

368 Evaporative enrichment increases δD and $\delta^{18}\text{O}$ values of leaf water relative to
369 xylem water. The δD_{leaf} is enriched relative to δD_{xylem} by $40 \pm 17\text{‰}$ in *B. nana* and $22 \pm$
370 16‰ in *E. vaginatum* (Fig. 4). The intersection between the leaf water δD - $\delta^{18}\text{O}$ line and
371 the LMWL can be used to infer the isotopic composition of source water for plant uptake
372 (Polissar and Freeman, 2010), and occurs at $\delta^{18}\text{O} = -19\text{‰}$ and $\delta\text{D} = -148\text{‰}$. This isotopic
373 composition lies between the July and August xylem water measurements.

374

375 3.2. Leaf waxes

376

377 3.2.1 Modern plant waxes

378 Leaves from both *B. nana* and *E. vaginatum* contain *n*-acids from C_{20} to C_{30} and
379 *n*-alkanes from C_{23} to C_{33} (Fig. 6). CPI results show a strong even-over-odd

380 predominance for *n*-acids for both *B. nana* and *E. vaginatum* ($\text{CPI}_{B. nana} = 14.2 \pm 2.8$;
381 $\text{CPI}_{E. vaginatum} = 6.3 \pm 1.5$) and vice versa for *n*-alkanes ($\text{CPI}_{B. nana} = 7.4 \pm 3.1$; $\text{CPI}_{E. vaginatum}$
382 $= 32.3 \pm 8.1$), reflecting the freshness of the sampled leaf waxes. Averaging all *B. nana*
383 samples, we find that even-chain *n*-acids are roughly equally distributed from C₂₂ to C₂₈,
384 whereas the *n*-alkane distribution has two peaks at C₂₇ and C₃₁. For C₂₀-C₃₀ *n*-acids, the
385 average chain length (ACL) is 24.5 ± 0.7 while for *n*-alkanes, the C₂₀-C₃₃ ACL averages
386 28.7 ± 0.4 . *E. vaginatum* lipids are, on average, unimodally distributed and dominated by
387 C₂₆ *n*-acid and C₃₁ *n*-alkane. ACL averages 24.8 ± 0.5 for *n*-acids and 30.1 ± 0.7 for *n*-
388 alkanes. No difference in ACL was observed between sampling months for either species
389 ($p = 0.59$ for *E. vaginatum* and $p = 0.16$ for *B. nana*). While *B. nana* and *E. vaginatum*
390 have similar concentrations of total *n*-alkanes ($1960 \mu\text{g g leaf}^{-1}$ and $1482 \mu\text{g g leaf}^{-1}$,
391 respectively; two-sample t-test $p = 0.167$), *B. nana* leaves contained significantly more *n*-
392 acids than *E. vaginatum* ($965 \mu\text{g g leaf}^{-1}$ and $142 \mu\text{g g leaf}^{-1}$, respectively; two-sample t-
393 test $p = 0.037$).

394 For isotopic analyses, we focus on the most abundant long chain *n*-acids (C₂₂-C₃₀)
395 and *n*-alkanes (C₂₅-C₃₁). Across all sampling periods, the $\delta\text{D}_{\text{wax}}$ of *B. nana* *n*-alkanes and
396 *n*-acids average -232‰ and -248‰ , respectively, while *E. vaginatum* *n*-alkanes and *n*-
397 acids average -305‰ and -278‰ , thus revealing discernible differences between plant
398 species, but inconsistent differences between lipid classes. Further differences are
399 apparent between homologues (Table 1 and Fig. 7). Calculations of ϵ_{app} from paired
400 measurements of xylem water and leaf waxes show that ϵ_{app} is more negative for leaf
401 waxes of *E. vaginatum* (*n*-alkane average: -182‰ , *n*-acid average: -154‰) than for
402 waxes of *B. nana* (*n*-alkane average: -89‰ , *n*-acid average: -106‰) (Table 1). The

403 difference in fractionation between the two species decreases with decreasing chain
404 length (Fig. 7). Furthermore, we note that ϵ_{app} is less negative during July than August
405 sampling, particularly for *E. vaginatum* (Fig. 5).

406

407 3.2.2 Sedimentary waxes

408 Sediment traps in Lake E5 collected between 0.05 and 0.3 grams of solids during
409 the deployment periods, equivalent to a mass flux of 0.1 to 0.85 g m⁻² d⁻¹. The
410 concentration of *n*-acids ($\Sigma\text{C}_{20}\text{-C}_{33}$) averaged 219 $\mu\text{g g sediment}^{-1}$, while the
411 concentration of *n*-alkanes ($\Sigma\text{C}_{20}\text{-C}_{33}$) averaged 248 $\mu\text{g g sediment}^{-1}$. The fluxes of
412 sediment, *n*-acids, and *n*-alkanes peak in June, during and shortly after the spring thaw
413 (Fig. 8), with values of 0.85 g m⁻² d⁻¹, 230 $\mu\text{g m}^{-2}$ d⁻¹, and 304 $\mu\text{g m}^{-2}$ d⁻¹, respectively.
414 The carbon preference index of sediment trap waxes ($\text{CPI}_{n\text{-acids}} = 2.7 \pm 1.3$; $\text{CPI}_{n\text{-alkanes}} =$
415 3.1 ± 2.9) are lower than the waxes from live vegetation, but still show strong even/odd
416 differences that reflect the relatively low degradation state of the waxes (Fig. 6). The *n*-
417 acids exhibit a unimodal distribution with a peak at the C₂₄ homologue and an ACL of
418 23.3 ± 0.7 . The *n*-alkanes are bimodal with peaks at C₂₀ and C₂₇, and have an ACL of
419 25.2 ± 1.5 . The low abundance of waxes required that sediment trap replicates be
420 composited into early and late summer samples for isotope analysis. In Lake E5, $\delta\text{D}_{\text{C}_{28}\text{-}}$
421 acid varies by 15‰ throughout the summer, ranging from -256‰ in May/June and
422 August/September to -243‰ in July (Fig. 8). The flux-weighted input of C₂₈ *n*-acid
423 during the summer has a δD value -253.7‰, which is indistinguishable from the C₂₈ *n*-
424 acid in Lake E5 surface sediment of -254.8‰.

425 In Toolik Lake, sediment flux and lipid fluxes were lower than in Lake E5, such
426 that wax abundance was too low for isotope analysis. The maximum sediment collected
427 was 0.05 g, and the maximum sediment flux was $0.05 \text{ g m}^{-2} \text{ d}^{-1}$. The concentration of *n*-
428 acids ($\text{C}_{20}\text{-C}_{30}$) averaged $226 \text{ } \mu\text{g g sediment}^{-1}$ while the concentration of *n*-alkanes ($\text{C}_{23}\text{-}$
429 C_{33}) averaged $438 \text{ } \mu\text{g g sediment}^{-1}$. Lipid distributions were similar between the two
430 lakes.

431 Like sediment trap samples, the C_{24} *n*-acid is the most abundant wax homologue
432 in surface sediments from all lakes. The ACL for *n*-acids is 24.8 ± 0.8 and the CPI is 5.2
433 ± 1.0 in the lake sediment samples, consistent with a terrestrial plant wax origin. The C_{27}
434 to C_{31} are the most abundant *n*-alkanes and present in roughly equal abundances. The
435 ACL and CPI for *n*-alkanes average 27.2 ± 0.4 and 5.0 ± 0.8 , respectively. Similar to
436 observations from the nearshore Beaufort Sea (Drenzek et al., 2007), *n*-acids are more
437 abundant than *n*-alkanes. The $\delta\text{D}_{\text{wax}}$ of lipids in surface sediments averages $-264.5 \pm$
438 7.1‰ for all measured *n*-alkanes and $-261.3 \pm 11.0\text{‰}$ for all measured *n*-acids and has a
439 range of 49‰ (Table 3) across all lakes and lipid homologues.

440 To calculate a watershed-scale ϵ_{app} , we compared the $\delta\text{D}_{\text{wax}}$ of lake surface
441 sediments from 24 lakes to the δD of plant source water. We provide three estimates of
442 ϵ_{app} , based on different estimates of $\delta\text{D}_{\text{source water}}$. Using precipitation-weighted mean
443 annual $\delta\text{D}_{\text{precipitation}}$ (-166‰), ϵ_{app} averages $-118 \pm 9\text{‰}$ for *n*-alkanes and $-114 \pm 13\text{‰}$ for
444 *n*-acids. Using precipitation-weighted mean summer $\delta\text{D}_{\text{precipitation}}$ (-139‰), ϵ_{app} averages -
445 $146 \pm 8\text{‰}$ for *n*-alkanes and $-142 \pm 13\text{‰}$ for *n*-acids. Using the average $\delta\text{D}_{\text{xylem}}$ values
446 measured in this study (-153‰), ϵ_{app} averages $-132 \pm 8\text{‰}$ for *n*-alkanes and $-128 \pm 13\text{‰}$
447 for *n*-acids. Values of ϵ_{app} tend to be slightly more negative for smaller carbon number

448 homologues than larger homologues (Fig. 7). Our estimates of sedimentary wax ϵ_{app}
449 suggest that *n*-alkanes are more strongly fractionated relative to source water than are *n*-
450 acids – the C₂₉ *n*-alkane is depleted by 15‰ relative to C₃₀ *n*-acid (paired t-test,
451 $p < 0.0001$), while C₂₇ *n*-alkane is just 4‰ depleted relative to C₂₈ *n*-acid (paired t-test,
452 $p = 0.060$). Thus while our plant samples exhibited opposing offsets between *n*-alkanes
453 and *n*-acids, the sedimentary waxes are in general agreement with expectations from
454 previous work on individual plants (Chikaraishi and Naraoka, 2007; Hou et al., 2007) and
455 marine sediments (Li et al., 2009).

456

457 3.3 Vegetation effects on apparent fractionation

458 Isotopic differences between study lakes most likely arise from watershed-scale
459 differences in soil water evaporation and/or plant distributions. Due to limited evidence
460 for evaporative fractionation observed in our soil samples, large observed differences in
461 ϵ_{app} between plant types, and the large variation in plant types across watersheds (Table
462 2), vegetation is likely the primary cause of the large ϵ_{app} variability (Table 2). Based on
463 single and multi-variate regressions, we find that the best predictor of ϵ_{app} for nearly all
464 wax homologues is the relative abundance of barren and dry tundra vegetation. While
465 barren tundra (bedrock) is dominated by lichens, the dry tundra is dominated by eudicot
466 shrubs and forbs such as *Salix spp.* The positive correlation is consistent with the
467 hypothesis that greater eudicot cover should result in less negative ϵ_{app} . In contrast, the
468 abundance of moist and shrub tundra, which contain an abundance of moss and the
469 sedges *Eriophorum spp.* and *Carex spp.*, is negatively correlated with ϵ_{app} (Fig. 9, Table
470 A2).

471

472 4. Discussion

473

474 4.1 Apparent fractionation in the Alaskan Arctic is similar to temperate and tropical 475 settings

476 A pressing question in the application of leaf wax hydrogen isotopes for
477 paleoclimate reconstructions is whether apparent D/H fractionation is affected by
478 enhanced transpiration in polar regions due to 24-hour photosynthesis, as suggested by
479 previous studies (Yang et al., 2011; Shanahan et al., 2013; Porter et al., 2016), or, if there
480 is little effect of latitude on ϵ_{app} as recently suggested by Liu et al. (2016). Our study site
481 is within the Arctic circle (68 °N), at a similar latitude to previous studies on sub-Arctic
482 and Arctic leaf wax fractionation, which are here considered those studies above 63 °N
483 (Sachse et al., 2006; Yang et al., 2011; Wilkie et al., 2012; Shanahan et al., 2013; Porter
484 et al., 2016). We find that ϵ_{app} of Arctic *n*-alkanes and *n*-acids are generally similar to
485 those observed at mid- and low-latitude locations (Sachse et al., 2004; Hou et al., 2007;
486 Garcin et al., 2012), suggesting that the effect of 24-hour photosynthesis is of limited
487 importance and that the fundamental controls on ϵ_{app} in the Arctic are similar to those in
488 temperate and tropical regions, with the exceptions that the Arctic is differentiated by its
489 extremely short growing season, unique flora, and the presence of permafrost.

490 With the exception of the study by Yang et al. (2011), our estimates of ϵ_{app} at the
491 plant scale are in general agreement with results from plants of the same growth forms
492 from regions both with and without a summer diel light cycle. For example, across a
493 latitudinal transect which included 24-hour daylight sites, Sachse et al. (2006) found that

494 *Betula pubescens* and *B. pendula* exhibited $\epsilon_{\text{alkane-water}}$ of -138 to -86‰, a range which
495 brackets our estimate of -108‰ for the closely related *B. nana*. Sachse et al. (2006) did
496 not observe a consistent latitudinal effect on ϵ_{app} within either *Betula* species, which
497 would also suggest day length has little effect on ϵ_{app} . The average *n*-acid D/H
498 fractionation for *B. nana* specimens at our site ($\epsilon_{\text{acid-water}} = -89\text{‰}$) falls within the range
499 reported for a variety of eudicot plants ($\epsilon_{\text{acid-water}} = -156$ to -85‰) collected from a mid-
500 latitude site in Massachusetts, USA by Hou et al. (2007). The Alaskan $\epsilon_{\text{alkane-water}}$ (-105‰)
501 is at least 10‰ enriched compared to Massachusetts specimens ($\epsilon_{\text{alkane-water}} = -180$ to -
502 115‰), and slightly enriched relative to the ϵ_{app} of -117‰ reported for C₂₇ *n*-alkanes of
503 dominant shrub taxa in western Greenland (Thomas et al., 2016). Fractionation values for
504 *E. vaginatum* ($\epsilon_{\text{alkane-water}} = -182\text{‰}$ and $\epsilon_{\text{acid-water}} = -153\text{‰}$) fall within the ranges for other
505 graminoids reported by Hou et al. (2007) ($\epsilon_{\text{alkane-water}} = -206$ - 154‰ and $\epsilon_{\text{acid-water}} = -195$ to
506 -148‰). Our results also overlap with ϵ_{app} measurements from living plants in Arctic
507 Siberia, where Wilkie et al. (2012) report ϵ_{app} values ranging from -135 to -97‰ for *n*-
508 acids from seven tundra species, comprising both eudicots and monocots. Unlike at our
509 sampling sites, however, Wilkie et al. (2012) did not observe a significant D-depletion in
510 monocots relative to eudicots. This between-site difference may arise because, while
511 *Eriophorum* in the Toolik Lake region is found primarily in mesic soils, *Poaceae*, the
512 monocot studied by Wilkie et al. (2012), can be found across diverse soil types in the
513 Arctic (Oswald et al., 2003) and may be more susceptible to evaporation effects on D/H
514 ratios.

515 In our study region, the ecosystem-scale ϵ_{app} inferred from waxes in lake
516 sediments averages -132‰ for *n*-alkanes and -128‰ for all *n*-acid homologues when the

517 average δD_{xylem} is used as a baseline for source water. The average source water δD value
518 is undoubtedly a mix of precipitation across seasons, and as discussed below, is likely
519 biased towards summer values in the Arctic. The δD_{xylem} values reported here represent a
520 snapshot in mid-summer and may be unique to the plant species studied here.
521 Nonetheless, because the soil thaw layer is shallow (<50 cm), plants are generally
522 drawing water from the same pool. The δD_{xylem} may also be enriched relative to xylem
523 waters in May/June when leaf flush occurs, thereby biasing ϵ_{app} to be slightly less
524 negative than the growing-season average. Nonetheless, the application of δD_{xylem} as an
525 estimate of source water is justified for a few reasons. First, the presence of some residual
526 cold season (D-depleted) water in soil profiles implies that mean summer $\delta D_{\text{precipitation}}$ as a
527 source water would over estimate $\delta D_{\text{source water}}$, while using a mean annual $\delta D_{\text{precipitation}}$
528 would likely underestimate $\delta D_{\text{source water}}$ because it would not account for the summer bias
529 in the growing season. Because the xylem water estimates fall intermediate between
530 mean annual and mean summer rainfall, we propose that the δD_{xylem} measurements
531 provide the most reasonable baseline value of the source water. While better constraining
532 the δD_{xylem} during the period of leaf flush would further aid the assessment of source
533 water seasonality, the δD_{wax} of newly formed leaves is more dependent on the D/H ratios
534 of stored carbohydrates and NADPH than on xylem waters (Newberry et al., 2015), and
535 so spring δD_{xylem} is not critical in this analysis.

536 The ecosystem-scale ϵ_{app} values are intermediate between our estimates of ϵ_{app}
537 from *B. nana* and *E. vaginatum*, and, for *n*-acids, slightly more negative than the ϵ_{app}
538 estimate of -110.5‰ in Arctic Siberia (Wilkie et al., 2012). The ϵ_{app} estimates for long

539 chain (C_{27} , C_{29} , C_{31}) *n*-alkanes in northern Alaska fall within the range of -141 to -122‰
540 found in high latitude lakes of Europe (Sachse et al., 2004). Our estimates are slightly
541 more negative than those reported from southern USA, where the C_{26} - C_{30} *n*-acids exhibit
542 ϵ_{app} values of -98 to -102‰ relative to precipitation (Hou et al., 2008), but more positive
543 than a report from West Africa, where ϵ_{app} for C_{29} and C_{31} *n*-alkanes was between -168
544 and -142‰. Regardless of the comparison with the tropics, our estimates are dramatically
545 more negative than the ϵ_{app} estimates of -55 to -60‰ for both *n*-alkanes and *n*-acids from
546 some prior work in sub-Arctic and Arctic sites (Shanahan et al., 2013; Porter et al., 2016).

547 We postulate that the large discrepancy in ϵ_{app} between our study and previous
548 Arctic field studies derives from differences in the assumed seasonality and estimated
549 isotope compositions of plant source waters. Some prior studies that found small Arctic
550 ϵ_{app} use source water δD values estimated to represent mean annual $\delta D_{precipitation}$ (Yang et
551 al., 2011; Shanahan et al., 2013; Porter et al., 2016). For the Baffin Island study
552 (Shanahan et al., 2013), this assumption is compounded with the use of estimated rather
553 than measured $\delta D_{precipitation}$ values, as well as low humidity and a predominance of
554 dicotyledonous species (forbs) in their study area, all of which might reduce apparent
555 D/H fractionation. In Central Canada, Porter et al. (2016) calculated ϵ_{app} of -59‰ by
556 comparing fossil waxes to mean annual precipitation preserved in pore ice. However, it is
557 unclear whether pore ice records water frozen *in situ* at the same time and in the same
558 season as that when the plant waxes were formed. Moreover, application of this ϵ_{app} value
559 to δD_{wax} of modern soils in their study area (Pautler et al., 2014) results in an
560 underestimation of modern mean annual $\delta D_{precipitation}$ by 28‰ and a resulting
561 underestimation of modern mean annual temperature by 13°C (Porter et al., 2016). While

562 it is possible that source water for plants can partially come from snowmelt (Alstad et al.,
563 1999; Leffler and Welker, 2013), the ground is often frozen during the season of snow
564 melt and water from snowmelt in Arctic spring is mostly lost through runoff. It is more
565 likely that the fossil pore water isotopes used by Porter et al. (2016) reflect cold season
566 (D-depleted) precipitation rather than precipitation during the plant growing season (D-
567 enriched) (Blok et al., 2015).

568 Low apparent fractionation values have been previously explained by the 24-hour
569 sunlit conditions that characterize the Arctic summer, which allow photosynthesis
570 throughout the 24-hour day that might drive strong isotopic fractionation of leaf waters
571 due to 24-hour evaporation. This hypothesis is supported by greenhouse experiments that
572 indicate ϵ_{app} values from -87 to -62‰ for plants grown in 24-hour light conditions (Yang
573 et al., 2009). These values are difficult to explain. It is possible that the exceptionally
574 small fractionation values that Yang et al. (2009) observed partly resulted from their
575 choice of study species – *Metasequoia*, *Larix*, and *Taxodium* are expected to exhibit
576 relatively small ϵ_{app} values based on their phylogenetic lineages (Gao et al., 2014a). Thus,
577 in cases where arctic forests are dominated by these conifers, a reduced fractionation
578 value may be appropriate for calculating ancient $\delta D_{precipitation}$ from ancient δD_{wax} .
579 Nonetheless, for the modern arctic tundra plants studied here, our data argue against a 24-
580 hour photosynthesis effect of leaf water isotopes.

581 Direct observations of $\epsilon_{leaf-xylem}$ do not indicate that continuous daylight has a
582 significant impact on δD_{wax} . Although evaporative enrichment at the leaf surface
583 increases δD_{leaf} relative to δD_{xylem} (Roden and Ehleringer, 1999; Tipple et al., 2015), the
584 magnitude of this enrichment observed at Toolik (40‰ and 21‰ for *B. nana* and *E.*

585 *vaginatum*, respectively) is within the range of isoscape model predictions for Alaska
586 (Kahmen et al., 2013a). The observed enrichment of leaf water over xylem water is also
587 similar to field and growth chamber observations in temperate environments
588 (Massachusetts and New York) with diel light cycles and relative humidity similar to
589 where Gao et al. (2014a) found that $\epsilon_{\text{leaf-xylem}}$ is slightly greater for eudicots ($34 \pm 13\%$)
590 than *Poales* ($20 \pm 11\%$). We hypothesize that the species difference in δD_{leaf} may result
591 from differences in plant height and leaf physiology, with *B. nana* somewhat taller and
592 more susceptible to leaf water enrichment due to a longer flow path of water during
593 transpiration (Gao and Huang, 2013). Regardless of the differences between plant types,
594 both plant water isotope measurements show little effect of continuous daylight on leaf
595 water isotopes, and by extension, net apparent fractionation.

596 While leaf water measurements are useful for assessing the importance of
597 evaporative enrichment, leaf waters can display large diel isotope variations (Flanagan
598 and Ehleringer, 1991) which were not captured in our sampling scheme. To circumvent
599 the uncertainties of spot sampling, we further tested the effect of changing leaf
600 transpiration on the isotope values of leaf water using the modified Craig-Gordon model
601 for leaf water (Flanagan and Ehleringer, 1991; Tipple et al., 2015). This model calculates
602 the isotopic composition of water at the site of evaporation, rather than water in the bulk
603 leaf tissue, which can also contain a fraction of unevaporated xylem water. Nevertheless,
604 the model can qualitatively describe the potential impact of diel or continuous
605 transpiration on leaf water isotope enrichment. Using average JJA meteorological
606 conditions from Toolik Field Station (Toolik Environmental Data Center Team, 2016),
607 and atmospheric vapor δD at Toolik (Klein et al., 2015), we modeled δD_{leaf} for the range

608 of transpiration rates of Arctic grasses (Gebauer et al., 1998). We find that δD_{leaf}
609 decreases with increasing transpiration rates, but the overall variation is small, less than
610 1‰ (Fig. 10). These model results support the findings of Sullivan and Welker (2007),
611 who demonstrated that, for arctic willow (*Salix arctica*), increasing transpiration results
612 in lower, not higher, leaf water $\delta^{18}\text{O}$. Furthermore, findings of Roden and Ehleringer
613 (1999) indicate that leaf water at the site of evaporation reaches isotopic equilibrium
614 within two hours under constant evaporation, and so prolonged (24 hour) transpiration
615 should not lead to anomalously enriched leaf water isotope values. Thus, our modeling
616 and prior observational data suggest that 24-hour transpiration in the Arctic would, if
617 anything, decrease δD_{leaf} and thereby make ϵ_{app} more negative, rather than the opposite.

618 Model results also suggest a relatively small humidity effect on leaf water
619 isotopes. For a 1% increase in relative humidity, δD_{leaf} decreases by 0.33‰ (Fig. 10).
620 Based on the $\delta D_{\text{precipitation}}$ -temperature relationship of $3.1\text{‰}\text{C}^{-1}$ reported by Porter et al.
621 (2016), this equates to approximately a 1 °C inferred temperature change per 10% change
622 in relative humidity. As such, the effect of humidity change on δD_{wax} interpretations may
623 be relatively insignificant in the Arctic.

624 The ϵ_{app} values for leaf waxes from *E. vaginatum* and *B. nana* align well with
625 previous studies that find waxes in graminoids are D-depleted relative to those from
626 forbs, shrubs, and trees (Sachse et al., 2012; Gao et al., 2014a; Liu et al., 2016) and that
627 waxes in monocots are depleted relative to eudicots (Gao et al., 2014a). Interestingly,
628 however, fractionation values for the shorter chain length *n*-acids (C_{24} and C_{26}) were
629 similar for our two study species. This result suggests that shorter chain lengths may be
630 more resilient to vegetation effects in the geologic record. However, with the knowledge

631 that other species, particularly *Sphagnum* moss (Nichols et al., 2009) and aquatic
632 macrophytes (Gao et al., 2011), contribute substantial C₂₄ *n*-acid and other short-chain
633 waxes to lake sediments, it remains uncertain if this finding can be extrapolated across all
634 relevant plant types.

635 It is possible that D/H fractionation in this study is overestimated (more negative
636 than true ϵ_{app}), due to seasonally biased sampling of waxes and source waters. To
637 evaluate this, we consider a wider range of possible source water δD values. For
638 sedimentary waxes in Toolik and the surrounding lakes, if the plant source water is equal
639 to the mean annual $\delta\text{D}_{\text{precipitation}}$ (-166‰) rather than summer xylem water (-153‰), ϵ_{app}
640 ranges from -99‰ for C₃₀ *n*-acid to -122‰ for C₂₂ and C₂₄ *n*-acids. This is still similar to
641 ϵ_{app} in non-polar regions (Sachse et al., 2004; Hou et al., 2008) and very different from
642 the small values observed at Baffin Island and Central Canada (Shanahan et al., 2013;
643 Porter et al., 2016). To generate ϵ_{app} as small as -60‰ at our site, it is necessary to invoke
644 source water δD values of -213‰. Such a strong winter-biased source water isotope
645 value is unlikely considering that $\delta\text{D}_{\text{xylem}}$ during the growing season averaged -153‰,
646 that 60% of annual precipitation occurs in the three summer months, and that most of the
647 snowmelt is lost as runoff during the spring thaw (Woo, 2012).

648

649 4.2 Constraining the seasonality of $\delta\text{D}_{\text{wax}}$ signals in the Arctic

650 It is challenging to accurately identify the isotope value of the source water
651 involved in plant wax synthesis in the Arctic because of the extreme seasonal changes in
652 $\delta\text{D}_{\text{precipitation}}$ and the uncertainty surrounding the timing of leaf wax synthesis. For our
653 location, we estimate that the δD of source water used for plant growth averages -153‰,

654 based upon both direct measurements of xylem water as well as the intersection between
655 the leaf evaporation line with the LMWL (Fig. 4). Although soil and xylem water
656 collections occurred during peak seasonal warmth and peak $\delta D_{\text{precipitation}}$, their isotopic
657 composition was intermediate between the mean annual amount-weighted $\delta D_{\text{precipitation}}$ (-
658 166‰) and the summer $\delta D_{\text{precipitation}}$ (JJA average = -139‰.) In regions of continuous
659 permafrost, soil infiltration of snowmelt is variable, but generally inhibited during cold
660 months by the impermeability of soil ice (Woo, 2012). As a result, considerable
661 snowmelt is lost as surface runoff and the spring/summer soil water during the period of
662 leaf flush is mostly composed of spring (May and June) precipitation. The predominance
663 of growing-season precipitation over cold-season precipitation in surface soil waters is
664 evident in both July and August, as the δD_{soil} is isotopically similar to spring and summer
665 rains (Fig. 4). Nevertheless, δD_{soil} increases from July to August, and, D-depleted water
666 is present at intermediate soil depths in July, which suggest that complete replacement of
667 remnant fall, winter, and spring precipitation requires several weeks to months and that
668 cold-season precipitation, or a mixture of cold- and growing season precipitation, may be
669 available for plant growth. The seasonal change in δD_{soil} profiles seems to have a stronger
670 influence on the δD_{xylem} of *Betula nana*, which as a shrub has a deeper rooting depth than
671 the sedge *Eriophorum vaginatum* (Fig. 5). Indeed, there are indications that snowmelt can
672 contribute over 30% of source water to plants (Ebbs, 2016). Nevertheless, xylem water
673 isotope measurements in this study and another study in Greenland (Sullivan and Welker,
674 2007) indicate that arctic plants primarily utilize water from the shallow, thawed soil
675 zones, where soil water is isotopically similar to growing season precipitation events
676 (Fig. 3).

677 The Lake E5 sediment trap results provide additional insight into seasonal
678 variations in the source water that plants use for biosynthesis (Fig. 8). Since the highest
679 flux of waxes to the sediment occurs during the spring freshet, we suggest that waxes
680 entering the lake are primarily produced during previous year(s) and are flushed from soil
681 by snowmelt. There are reports from the Mackenzie River delta and other high-latitude
682 localities that waxes can be pre-aged by years to millennia at the time of deposition
683 (Drenzek et al., 2007). Considering the primary transport mechanism (particulate
684 transport via snowmelt) and lack of degradation inferred from CPI values, we suspect that
685 the majority of waxes entering the lake can be considered recent. The leaf litter reflects
686 the complex integration of the seasonal production, isotopic evolution, and ablation, of
687 waxes from a variety of species. Importantly, the amplitude of the sediment trap δD_{wax}
688 variability throughout the summer (15‰) is greater than we observed in the monthly
689 change in δD_{wax} of living plants, which is surprising, but may be because we did not
690 measure δD_{wax} of plants in the earliest part of the growing season (May or June).

691 Despite the enrichment of xylem water in August relative to July, δD_{wax} of plants
692 did not change between July and August (Fig. 5). To explain the stable δD_{wax} values,
693 there are multiple plausible scenarios. First, *de novo* wax biosynthesis may have occurred
694 only during the brief period of leaf flush, which occurs in mid-June at our site, as has
695 been reported from greenhouse studies of *Populus trichocarpa* (Kahmen et al., 2011). If
696 this is the case, δD_{wax} would be insensitive to seasonal change in δD_{xylem} ; in field settings,
697 however, weeks to months are required for δD_{wax} to stabilize (Newberry et al., 2015)
698 because of a greater need to replenish lost waxes in more harsh conditions. The Lake E5

699 sediment trap results show seasonal changes in δD_{wax} , implying some seasonal
700 regeneration of waxes (Fig. 8).

701 In the process of *de novo* wax regeneration during the growing season, δD_{wax} and
702 biosynthetic fractionation at the time of budbreak tend to be less negative than during
703 mid/late-summer because of a greater contribution of D-enriched material from the
704 recycling of stored carbohydrates early in the season (Newberry et al., 2015).
705 Biosynthetic changes during the growing season are also reported to depress mid-summer
706 D/H ratios in saltmarshes (Sessions, 2006). As such, a second plausible scenario to
707 explain the seasonal progression of sediment trap waxes relative to living plant waxes is
708 that spring (June) waxes at our site were more D-enriched than the late-summer waxes,
709 similar to what Newberry et al. (2015) observed in the UK. This model of seasonal δD_{wax}
710 progression resolves the discrepancy between our leaf and sediment trap samples. That is,
711 waxes entering the lake in mid-summer (July), when δD_{wax} was at a maximum, were
712 likely produced during spring (mid-June), when biosynthetic fractionation is minimal. As
713 the initial waxes were ablated over the weeks following budbreak, they were replaced by
714 more D-depleted waxes, despite increasingly D-enriched xylem waters. δD_{wax} was then
715 relatively stable during our limited sampling window between July and August. This
716 hypothesis is most parsimonious with the relatively D-depleted waxes which enter the
717 lake in late fall and during the spring freshet because the waxes overwintering on land are
718 somewhat depleted relative to the early season waxes and would have been derived from
719 litterfall originating in August and September. We cannot confirm this hypothesis without
720 further sampling May/June leaves. Nonetheless, this point argues for a mixed-season,
721 summer biased precipitation source.

722 An alternative explanation for the seasonal cycle in sediment trap δD_{wax} is that a
723 subset of plant species on the landscape produce a relatively large quantity of D-enriched
724 waxes during mid-summer, but these waxes do not contribute substantially to the
725 soil/particular leaf matter washed into the lake in spring. If this is the case, our vegetation
726 survey was not broad enough to observe these plant types.

727 Overall, our observations support the hypothesis that δD of long chain *n*-acids and
728 *n*-alkanes records a summer-biased mean annual precipitation isotope signal in the Arctic.
729 Wilkie et al. (2012) found that the isotopic composition of spring precipitation and
730 streamwater is a good representation of plant source water during the growing season in
731 Siberia. In their study the streamwater isotope values were intermediate between mean
732 annual and summer precipitation values, and the resulting value of ϵ_{app} was
733 approximately -105‰. We find strong evidence that plants use summer precipitation in
734 the Toolik region, and to a lesser extent, fall and winter precipitation stored in the soil.
735 However, we note that the average composition of plant source waters is similar to
736 $\delta D_{\text{precipitation}}$ during spring (May and June). The use of summer precipitation by plants was
737 also observed in Arctic Svalbard, where the δD of plant annual growth rings is more
738 strongly correlated with summer $\delta D_{\text{precipitation}}$ than with either winter $\delta D_{\text{precipitation}}$ or with
739 the amount of snow accumulation during winter (Blok et al., 2015). These findings have
740 important implications for the interpretation of δD_{wax} records of Arctic paleoclimate,
741 given the potential importance of seasonality in governing high-latitude climate change
742 (Denton et al., 2005).

743

744 4.3 Constraining landscape-scale vegetation effects on sedimentary δD_{wax}

745 Surface sediment δD_{wax} varies by up to 37‰ across our 24 study lakes for a given
746 *n*-acid homologue and by up to 32‰ for a given *n*-alkane homologue. These ranges are
747 substantial, especially if δD_{wax} is to be used for reconstructing paleoclimate – 37‰ is
748 equivalent to $\sim 12^{\circ}\text{C}$ of temperature variability based on the modern relationship between
749 temperature and $\delta D_{\text{precipitation}}$ of $\sim 3.1\text{‰ }^{\circ}\text{C}^{-1}$ across northern North America (Porter et al.,
750 2016). In the absence of climatic and $\delta D_{\text{precipitation}}$ gradients in our constrained study area,
751 we assume that the variability arises principally from local (watershed-scale) variations in
752 vegetation. Quantifying the vegetation effect is therefore important because in Alaska and
753 around the Arctic, deglacial and modern climate warming have been accompanied by
754 vegetation changes, especially an expansion of shrub vegetation (Livingstone, 1955; Tape
755 et al., 2012), which could alter the ecosystem value of ϵ_{app} and impact reconstructions of
756 past $\delta D_{\text{precipitation}}$.

757 The different glacial landscapes in the Toolik Lake area support diverse and well-
758 characterized vegetation assemblages with varying relative abundances of monocot and
759 eudicot plants over a very small area (Walker et al., 1994), allowing a test of whether
760 catchment-scale differences in vegetation affect δD_{wax} independent of climatic influences.
761 In general, we find that for lakes situated in watersheds with a high abundance of dry and
762 barren tundra, δD_{wax} is 10-30‰ less negative than for those lakes surrounded by sedge
763 and grass-dominated vegetation classes such as moist acidic tundra and wetlands.

764 Of the nine vegetation classes defined by Walker and Maier (2008), dry tundra
765 and barren/heath tundra are the two classes with the least abundance of monocots. The
766 vegetation in these units predominantly support lichens, dicotyledonous forbs and
767 prostrate shrubs such as *Salix reticulata*. Based on the ϵ_{app} difference between *E*.

768 *vaginatum* and *B. nana* in this study and the previously well-described difference
769 between monocots and dicots (Gao et al., 2014a), we expect waxes in lakes surrounded
770 predominantly by dry tundra to be relatively D-enriched. In contrast, wetland areas and
771 moist tundra contain a mix of shrubs, forbs, monocotyledonous graminoids (ex.
772 *Eriophorum spp.* and *Carex spp.*), and *Sphagnum* moss, with graminoids and mosses
773 dominating the biomass (Walker et al., 1994) and so lake sediments in this setting should
774 be relatively D-depleted.

775 While the vegetation classes are blunt instruments for describing species
776 assemblages, the correlations observed here (Fig. 9, Table A2) are consistent with a
777 vegetation effect. Our study is limited in that we did not track soil and or plant water D/H
778 values from dry tundra ecotypes, and it is possible that differences in δD_{soil} also
779 contributes to the positive relationship of ϵ_{app} with abundance of dry tundra. Evaporative
780 effects are expected to be small based on our soil water isotope measurements from moist
781 acidic tundra (Fig. 4). However, the extremely shallow organic soils in the dry/barren
782 tundra could result in short soil water residence time, such that δD_{soil} ratios would closely
783 track the seasonal pattern in $\delta D_{\text{precipitation}}$, and the contribution of winter precipitation (D-
784 depleted) to soil water is relatively small. Whether δD_{soil} differs across land cover types
785 or not, we suggest that the predominance of eudicots on the dry tundra influences the
786 δD_{wax} we observe in lake sediments via the lower ϵ_{app} values that characterize eudicot
787 vegetation.

788 Watershed scale vegetation effects should be most prominent if waxes are
789 primarily transported through runoff, and least prominent if aeolian transport prevails, as
790 the latter should result in exchange of waxes between watersheds and reduced variability

791 across lakes. While waxes can be transported via wind over long ranges as aerosols
792 (Conte and Weber, 2002; Gao et al., 2014b; Nelson et al., 2017) or particulates
793 (Fahnestock et al., 2000), the large range in sediment δD_{wax} observed among our study
794 lakes suggests that hydraulic transport causes the lake sediment δD_{wax} signal to primarily
795 record watershed scale effects of vegetation and soil. Local transport is further
796 substantiated by the seasonal pattern in wax transport and deposition observed in the lake
797 sediment traps. Approximately 65% of the total *n*-acids (C₂₀-C₃₀) were deposited between
798 May 16 and July 1, during the spring freshet for Arctic lakes. The most likely explanation
799 for this peak is that waxes are transported by runoff during the period of high snowmelt
800 and mass movement. A predominance of local hydrologic transport contrasts with that of
801 temperate European lakes, where Nelson et al. (2017) find that aeolian transport is most
802 important. The difference could arise because the short stature of Arctic vegetation limits
803 windborne material, or because the snowmelt runoff event is more intense in our study
804 lake catchments than in the European lake catchments. As the summer progresses and
805 snowmelt-derived inputs decline, long-distance aerosol waxes may become more
806 important relative to local hydraulic inputs. Since the late summer wax flux is small,
807 however, watershed scale heterogeneity is preserved in lake sediments.

808 Overall, the range in the ecosystem scale ϵ_{app} between lakes is substantially
809 smaller than the potential range based on end-member monocot and eudicot
810 fractionations that we found at the plant scale. The reduced range could be due to some
811 aerosol transport homogenizing the isotope signal between lakes, or simply because
812 within each watershed, plant communities contain a mixture of monocot and eudicot
813 species, and true monocot/dicot end-members are never achieved at the watershed scale.

814 It is evident, based on the scatter in the ϵ_{app} – vegetation relationship and on the different
815 lipid distributions between *E. vaginatum*, *B. nana*, and the surface sediment waxes, that
816 other plant species contribute a considerable portion of the sedimentary waxes. Thus,
817 while our study species may provide a reasonable representation of two major plant
818 classes, they do not completely capture the variability in δD_{wax} of the contributing tundra
819 plants. In particular, the sedimentary waxes are characterized by dominant chain lengths
820 of C_{27} *n*-alkane and C_{24} *n*-acid, a feature not observed in either study species. A survey of
821 all tundra plant types will help further refine vegetation-based ϵ_{app} correction methods.
822 Nonetheless, the impact of vegetation assemblages is consistent with expectations based
823 on fractionation among plant types. These data stress the importance of considering
824 independent estimates of paleovegetation, such as pollen (Feakins, 2013) or plant
825 macrofossils (Nichols et al., 2014) when quantitatively determining Arctic $\delta D_{\text{precipitation}}$
826 based on sediment or soil δD_{wax} measurements.

827

828 5. Conclusions

829 Here we assessed the effects of water uptake, transpiration, biosynthesis, and
830 landscape integration as controls on the D/H fractionation associated with leaf wax
831 formation in Arctic Alaska, and provide estimates of ϵ_{app} under different vegetation
832 regimes.

833 We find that ϵ_{app} values of two of the most abundant plants in the Arctic tundra,
834 *B. nana* and *E. vaginatum*, are similar to shrubs and grasses in non-Arctic sites. This
835 finding is substantiated by direct observations of leaf water isotope enrichment and ϵ_{app} at
836 the plant-scale as well as ϵ_{app} at the ecosystem-scale. Likewise, modeled leaf water shows

837 no particularly strong enrichment in a continuous light regime. We propose that the effect
838 of prolonged, 24-hour photosynthesis during the Arctic summer on the isotopic
839 composition of waxes is small in the low Arctic tundra despite 24-hour day lengths.

840 We take advantage of the strong edaphic control on vegetation assemblages in the
841 Brooks Range foothills to produce the first analysis of a vegetation effect on ϵ_{app} in the
842 absence of a climatic gradient. Across 24 lakes within 10 km of each other, ϵ_{app} varied by
843 44‰. This result suggests that 1) wax transport between watersheds as aerosols is small
844 compared to the hydraulic transport within watersheds and 2) variation in plant
845 assemblages between watersheds plays a significant role in the observed ϵ_{app} . Using
846 vegetation maps, we demonstrate a positive correlation between the abundance of dry
847 tundra (eudicots) and ϵ_{app} for long-chain *n*-acids and *n*-alkanes. The relationship
848 illustrates the necessity of correcting δD_{wax} changes for changes in vegetation, and serves
849 as a guide for such corrections. We propose that for sedimentary records of δD_{wax} , a
850 sliding scale of ϵ_{app} can be appropriately applied if the relative abundance of eudicots is
851 known.

852

853

854 Acknowledgements

855

856 Thanks to Alice Carter, Dan White, and William Longo for assistance with field
857 collection. Joe Orchardo, Rafael Tarozo, and Josue Crowther helped with laboratory
858 analyses. This work was supported by the ARC LTER (NSF-DEB-1026843), NSF OPP
859 award (1503846), the Brown-MBL joint graduate program, and research grants to Will
860 Daniels from the Geologic Society of American and the Institute at Brown in
861 Environment and Society. The Toolik Lake precipitation isotope data is partially
862 supported by J. Welker's NSF OPP MRI award (0953271) and the Alaska Water Isotope
863 Network (AKWIN).

864

865

- 867 Alstad, K., Welker, J., Williams, S. and Trlica, M. (1999) Carbon and water relations of
868 *Salix monticola* in response to winter browsing and changes in surface water
869 hydrology: an isotopic study using $\delta^{13}\text{C}$ and $\delta^{18}\text{O}$. *Oecologia* 120, 375-385.
- 870 Blok, D., Weijers, S., Welker, J.M., Cooper, E.J., Michelsen, A., Löffler, J. and Elberling,
871 B. (2015) Deepened winter snow increases stem growth and alters stem $\delta^{13}\text{C}$ and
872 $\delta^{15}\text{N}$ in evergreen dwarf shrub *Cassiope tetragona* in high-arctic Svalbard tundra.
873 *Environmental Research Letters* 10, 044008.
- 874 Bowen, G. (2015) The Online Isotopes in Precipitation Calculator, version 2.2.
875 <http://www.waterisotopes.org>.
- 876 Bowen, G.J. and Revenaugh, J. (2003) Interpolating the isotopic composition of
877 modern meteoric precipitation. *Water Resour. Res.* 39, 1299.
- 878 Bray, E. and Evans, E. (1961) Distribution of n-paraffins as a clue to recognition of
879 source beds. *Geochim. Cosmochim. Acta* 22, 2-15.
- 880 CAVM Team (2003) Circumpolar Arctic Vegetation Map. Scale 1:7,500,000.
881 Conservation of Arctic Flora and Fauna (CAFF) Map No. 1. U.S. Fish and Wildlife
882 Service, Anchorage, Alaska.
- 883 Chapin III, F.S., Shaver, G.R., Giblin, A.E., Nadelhoffer, K.J. and Laundre, J.A. (1995)
884 Responses of arctic tundra to experimental and observed changes in climate.
885 *Ecology* 76, 694-711.
- 886 Cherry, J.E., Déry, S.J., Stieglitz, M. and Pan, F.-f. (2014) Meteorology and climate of
887 Toolik Lake and the north slope of Alaska: Past, present and future. *Alaska's*
888 *changing Arctic: Ecological consequences for tundra, streams, and lakes*. Oxford
889 Univ. Press.
- 890 Chikaraishi, Y. and Naraoka, H. (2007) $\delta^{13}\text{C}$ and δD relationships among three n-
891 alkyl compound classes (n-alkanoic acid, n-alkane and n-alkanol) of terrestrial
892 higher plants. *Org. Geochem.* 38, 198-215.
- 893 Chikaraishi, Y., Naraoka, H. and Poulson, S.R. (2004) Hydrogen and carbon isotopic
894 fractionations of lipid biosynthesis among terrestrial (C3, C4 and CAM) and aquatic
895 plants. *Phytochemistry* 65, 1369-1381.
- 896 Conte, M.H. and Weber, J.C. (2002) Plant biomarkers in aerosols record isotopic
897 discrimination of terrestrial photosynthesis. *Nature* 417, 639-641.
- 898 Dansgaard, W. (1964) Stable isotopes in precipitation. *Tellus* 16, 436-468.
- 899 Denton, G., Alley, R., Comer, G. and Broecker, W. (2005) The role of seasonality in
900 abrupt climate change. *Quaternary Science Reviews* 24, 1159-1182.
- 901 Drenzek, N.J., Montluçon, D.B., Yunker, M.B., Macdonald, R.W. and Eglinton, T.I.
902 (2007) Constraints on the origin of sedimentary organic carbon in the Beaufort Sea
903 from coupled molecular ^{13}C and ^{14}C measurements. *Mar. Chem.* 103, 146-162.
- 904 Ebbs, L. (2016) Response of Arctic shrubs to deeper winter snow is species and
905 ecosystem dependent: an isotopic study in northern Alaska. Thesis.
- 906 Ehleringer, J. and Dawson, T. (1992) Water uptake by plants: perspectives from
907 stable isotope composition. *Plant, Cell Environ.* 15, 1073-1082.
- 908 Fahnestock, J., Povirk, K. and Welker, J. (2000) Abiotic and biotic effects of increased
909 litter accumulation in arctic tundra. *Ecography* 23, 623-631.

910 Feakins, S.J. (2013) Pollen-corrected leaf wax D/H reconstructions of northeast
911 African hydrological changes during the late Miocene. *Palaeogeogr., Palaeoclimatol.,*
912 *Palaeoecol.* 374, 62-71.

913 Feakins, S.J., Warny, S. and Lee, J.-E. (2012) Hydrologic cycling over Antarctica
914 during the middle Miocene warming. *Nature Geoscience* 5, 557-560.

915 Flanagan, L.B. and Ehleringer, J.R. (1991) Effects of Mild Water Stress and Diurnal
916 Changes in Temperature and Humidity on the Stable Oxygen and Hydrogen Isotopic
917 Composition of Leaf Water in *Cornus stolonifera* L. *Plant Physiol.* 97, 298-305.

918 Gao, L., Burnier, A. and Huang, Y. (2012) Quantifying instantaneous regeneration
919 rates of plant leaf waxes using stable hydrogen isotope labeling. *Rapid Commun.*
920 *Mass Spectrom.* 26, 115-122.

921 Gao, L., Edwards, E.J., Zeng, Y. and Huang, Y. (2014a) Major Evolutionary Trends in
922 Hydrogen Isotope Fractionation of Vascular Plant Leaf Waxes. *PLoS ONE* 9,
923 e112610.

924 Gao, L., Hou, J., Toney, J., MacDonald, D. and Huang, Y. (2011) Mathematical modeling
925 of the aquatic macrophyte inputs of mid-chain n-alkyl lipids to lake sediments:
926 implications for interpreting compound specific hydrogen isotopic records.
927 *Geochimica et Cosmochimica Acta* 75, 3781-3791.

928 Gao, L. and Huang, Y. (2013) Inverse gradients in leaf wax δD and $\delta^{13}C$ values along
929 grass blades of *Miscanthus sinensis*: Implications for leaf wax reproduction and
930 plant physiology. *Oecologia* 172, 347-357.

931 Gao, L., Zheng, M., Fraser, M. and Huang, Y. (2014b) Comparable hydrogen isotopic
932 fractionation of plant leaf wax n - alkanolic acids in arid and humid subtropical
933 ecosystems. *Geochem. Geophys. Geosyst.* 15, 361-373.

934 Garcin, Y., Schwab, V.F., Gleixner, G., Kahmen, A., Todou, G., Séné, O., Onana, J.-M.,
935 Achoundong, G. and Sachse, D. (2012) Hydrogen isotope ratios of lacustrine
936 sedimentary n-alkanes as proxies of tropical African hydrology: insights from a
937 calibration transect across Cameroon. *Geochim. Cosmochim. Acta* 79, 106-126.

938 Gebauer, R., Reynolds, J. and Tenhunen, J. (1998) Diurnal patterns of CO₂ and H₂O
939 exchange of the Arctic sedges *Eriophorum angustifolium* and *E. vaginatum*
940 (Cyperaceae). *Am. J. Bot.* 85, 592-592.

941 Hamilton, T.D. (2003) Surficial geology of the Dalton Highway (Iktillik-
942 Sagavanirktok rivers) area, southern Arctic foothills, Alaska.

943 Hou, J., D'Andrea, W.J. and Huang, Y. (2008) Can sedimentary leaf waxes record D/H
944 ratios of continental precipitation? Field, model, and experimental assessments.
945 *Geochim. Cosmochim. Acta* 72, 3503-3517.

946 Hou, J., D'Andrea, W.J., MacDonald, D. and Huang, Y. (2007) Hydrogen isotopic
947 variability in leaf waxes among terrestrial and aquatic plants around Blood Pond,
948 Massachusetts (USA). *Org. Geochem.* 38, 977-984.

949 Huang, Y., Shuman, B., Wang, Y. and Webb, T. (2004) Hydrogen isotope ratios of
950 individual lipids in lake sediments as novel tracers of climatic and environmental
951 change: a surface sediment test. *J. Paleolimnol.* 31, 363-375.

952 Jasechko, S., Lechler, A., Pausata, F., Fawcett, P., Gleeson, T., Cendón, D., Galewsky, J.,
953 LeGrande, A., Risi, C. and Sharp, Z. (2015) Glacial-interglacial shifts in global and
954 regional precipitation $\delta^{18}O$. *Clim. Past Discuss* 11, 831-872.

955 Kahmen, A., Dawson, T.E., Vieth, A. and Sachse, D. (2011) Leaf wax n - alkane δD
956 values are determined early in the ontogeny of *Populus trichocarpa* leaves when
957 grown under controlled environmental conditions. *Plant, Cell Environ.* 34, 1639-
958 1651.

959 Kahmen, A., Hoffmann, B., Schefuß, E., Arndt, S.K., Cernusak, L.A., West, J.B. and
960 Sachse, D. (2013a) Leaf water deuterium enrichment shapes leaf wax n-alkane δD
961 values of angiosperm plants II: Observational evidence and global implications.
962 *Geochim. Cosmochim. Acta* 111, 50-63.

963 Kahmen, A., Schefuß, E. and Sachse, D. (2013b) Leaf water deuterium enrichment
964 shapes leaf wax n-alkane δD values of angiosperm plants I: Experimental evidence
965 and mechanistic insights. *Geochim. Cosmochim. Acta* 111, 39-49.

966 Klein, E., Nolan, M., McConnell, J., Sigl, M., Cherry, J., Young, J. and Welker, J. (2016)
967 McCall Glacier record of Arctic climate change: Interpreting a northern Alaska ice
968 core with regional water isotopes. *Quaternary Science Reviews* 131, 274-284.

969 Klein, E.S., Cherry, J.E., Young, J., Noone, D., Leffler, A.J. and Welker, J.M. (2015) Arctic
970 cyclone water vapor isotopes support past sea ice retreat recorded in Greenland ice.
971 *Scientific Reports* 5, 10295.

972 Konecky, B., Russell, J. and Bijaksana, S. (2016) Glacial aridity in central Indonesia
973 coeval with intensified monsoon circulation. *Earth. Planet. Sci. Lett.* 437, 15-24.

974 Leffler, A.J. and Welker, J.M. (2013) Long-term increases in snow pack elevate leaf N
975 and photosynthesis in *Salix arctica*: responses to a snow fence experiment in the
976 High Arctic of NW Greenland. *Environmental Research Letters* 8, 025023.

977 Li, C., Sessions, A.L., Kinnaman, F.S. and Valentine, D.L. (2009) Hydrogen-isotopic
978 variability in lipids from Santa Barbara Basin sediments. *Geochim. Cosmochim. Acta*
979 73, 4803-4823.

980 Liu, J., Liu, W., An, Z. and Yang, H. (2016) Different hydrogen isotope fractionations
981 during lipid formation in higher plants: Implications for paleohydrology
982 reconstruction at a global scale. *Scientific Reports* 6, 19711.

983 Livingstone, D. (1955) Some pollen profiles from arctic Alaska. *Ecology*, 587-600.

984 Longo, W.M., Theroux, S., Giblin, A.E., Zheng, Y., Dillon, J.T. and Huang, Y. (2016)
985 Temperature calibration and phylogenetically distinct distributions for freshwater
986 alkenones: Evidence from northern Alaskan lakes. *Geochim. Cosmochim. Acta* 180,
987 177-196.

988 Nelson, D.B., Knohl, A., Sachse, D., Schefuß, E. and Kahmen, A. (2017) Sources and
989 abundances of leaf waxes in aerosols in central Europe. *Geochim. Cosmochim. Acta*
990 198, 299-314.

991 Newberry, S.L., Kahmen, A., Dennis, P. and Grant, A. (2015) n-Alkane biosynthetic
992 hydrogen isotope fractionation is not constant throughout the growing season in the
993 riparian tree *Salix viminalis*. *Geochim. Cosmochim. Acta* 165, 75-85.

994 Nichols, J.E., Peteet, D.M., Moy, C.M., Castañeda, I.S., McGeachy, A. and Perez, M.
995 (2014) Impacts of climate and vegetation change on carbon accumulation in a
996 south-central Alaskan peatland assessed with novel organic geochemical
997 techniques. *The Holocene* 24, 1146-1155.

998 Nichols, J.E., Walcott, M., Bradley, R., Pilcher, J. and Huang, Y. (2009) Quantitative
999 assessment of precipitation seasonality and summer surface wetness using

1000 ombrotrophic sediments from an Arctic Norwegian peatland. *Quatern. Res.* 72, 443-
1001 451.

1002 Niedermeyer, E.M., Forrest, M., Beckmann, B., Sessions, A.L., Mulch, A. and Schefuß,
1003 E. (2016) The stable hydrogen isotopic composition of sedimentary plant waxes as
1004 quantitative proxy for rainfall in the West African Sahel. *Geochim. Cosmochim. Acta*
1005 184, 55-70.

1006 Oswald, W.W., Brubaker, L.B., Hu, F.S. and Gavin, D.G. (2003) Pollen - vegetation
1007 calibration for tundra communities in the Arctic Foothills, northern Alaska. *J. Ecol.*
1008 91, 1022-1033.

1009 Pagani, M., Pedentchouk, N., Huber, M., Sluijs, A., Schouten, S., Brinkhuis, H., Damsté,
1010 J.S.S. and Dickens, G.R. (2006) Arctic hydrology during global warming at the
1011 Palaeocene/Eocene thermal maximum. *Nature* 442, 671-675.

1012 Pautler, B.G., Reichart, G.-J., Sanborn, P.T., Simpson, M.J. and Weijers, J.W. (2014)
1013 Comparison of soil derived tetraether membrane lipid distributions and plant-wax
1014 δD compositions for reconstruction of Canadian Arctic temperatures. *Palaeogeogr.,*
1015 *Palaeoclimatol., Palaeoecol.* 404, 78-88.

1016 Polissar, P.J. and Freeman, K.H. (2010) Effects of aridity and vegetation on plant-wax
1017 δD in modern lake sediments. *Geochim. Cosmochim. Acta* 74, 5785-5797.

1018 Porter, T.J., Froese, D.G., Feakins, S.J., Bindeman, I.N., Mahony, M.E., Pautler, B.G.,
1019 Reichart, G.-J., Sanborn, P.T., Simpson, M.J. and Weijers, J.W.H. (2016) Multiple water
1020 isotope proxy reconstruction of extremely low last glacial temperatures in Eastern
1021 Beringia (Western Arctic). *Quaternary Science Reviews* 137, 113-125.

1022 Roden, J.S. and Ehleringer, J.R. (1999) Observations of hydrogen and oxygen
1023 isotopes in leaf water confirm the Craig-Gordon model under wide-ranging
1024 environmental conditions. *Plant Physiol.* 120, 1165-1174.

1025 Sachse, D., Billault, I., Bowen, G.J., Chikaraishi, Y., Dawson, T.E., Feakins, S.J., Freeman,
1026 K.H., Magill, C.R., McInerney, F.A. and Van der Meer, M.T. (2012) Molecular
1027 paleohydrology: interpreting the hydrogen-isotopic composition of lipid biomarkers
1028 from photosynthesizing organisms. *Annual Review of Earth and Planetary Sciences*
1029 40, 221-249.

1030 Sachse, D., Gleixner, G., Wilkes, H. and Kahmen, A. (2010) Leaf wax n-alkane δD
1031 values of field-grown barley reflect leaf water δD values at the time of leaf
1032 formation. *Geochim. Cosmochim. Acta* 74, 6741-6750.

1033 Sachse, D., Radke, J. and Gleixner, G. (2004) Hydrogen isotope ratios of recent
1034 lacustrine sedimentary n-alkanes record modern climate variability. *Geochim.*
1035 *Cosmochim. Acta* 68, 4877-4889.

1036 Sachse, D., Radke, J. and Gleixner, G. (2006) δD values of individual n-alkanes from
1037 terrestrial plants along a climatic gradient—Implications for the sedimentary
1038 biomarker record. *Org. Geochem.* 37, 469-483.

1039 Sauer, P.E., Eglinton, T.I., Hayes, J.M., Schimmelmann, A. and Sessions, A.L. (2001)
1040 Compound-specific D/H ratios of lipid biomarkers from sediments as a proxy for
1041 environmental and climatic conditions. *Geochim. Cosmochim. Acta* 65, 213-222.

1042 Sessions, A.L. (2006) Seasonal changes in D/H fractionation accompanying lipid
1043 biosynthesis in *Spartina alterniflora*. *Geochim. Cosmochim. Acta* 70, 2153-2162.

1044 Sessions, A.L., Burgoyne, T.W., Schimmelmann, A. and Hayes, J.M. (1999)
1045 Fractionation of hydrogen isotopes in lipid biosynthesis. *Org. Geochem.* 30, 1193-
1046 1200.

1047 Shanahan, T., Huguen, K., Ampel, L., Sauer, P. and Fornace, K. (2013) Environmental
1048 controls on the $^{2}H/^{1}H$ values of terrestrial leaf waxes
1049 in the Eastern Canadian Arctic. *Geochim. Cosmochim. Acta.*

1050 Shaver, G.R., Laundre, J.A., Bret-Harte, M.S., Chapin III, F.S., Mercado-Díaz, J.A., Giblin,
1051 A.E., Gough, L., Gould, W.A., Hobbie, S.E. and Kling, G.W. (2014) Terrestrial
1052 Ecosystems at Toolik Lake, Alaska. *Alaska's Changing Arctic: Ecological*
1053 *Consequences for Tundra, Streams and Lakes*, Oxford University Press, New York,
1054 90-142.

1055 Smith, F.A. and Freeman, K.H. (2006) Influence of physiology and climate on δD
1056 of leaf wax n -alkanes from C_3 and C_4
1057 grasses. *Geochim. Cosmochim. Acta* 70, 1172-1187.

1058 Sternberg, L.d.S.L. (1988) D/H ratios of environmental water recorded by D/H ratios
1059 of plant lipids. *Nature* 333, 59-61.

1060 Sullivan, P.F. and Welker, J.M. (2007) Variation in leaf physiology of *Salix arctica*
1061 within and across ecosystems in the High Arctic: test of a dual isotope ($\Delta^{13}C$ and
1062 $\Delta^{18}O$) conceptual model. *Oecologia* 151, 372-386.

1063 Tape, K.D., Hallinger, M., Welker, J.M. and Ruess, R.W. (2012) Landscape
1064 heterogeneity of shrub expansion in Arctic Alaska. *Ecosystems* 15, 711-724.

1065 Thomas, E.K., Briner, J.P., Ryan - Henry, J.J. and Huang, Y. (2016) A major increase in
1066 winter snowfall during the middle Holocene on western Greenland caused by
1067 reduced sea ice in Baffin Bay and the Labrador Sea. *Geophys. Res. Lett.* 43, 5302-
1068 5308.

1069 Thomas, E.K., McGrane, S., Briner, J.P. and Huang, Y. (2012) Leaf wax δ^2H and
1070 varve-thickness climate proxies from proglacial lake sediments, Baffin Island, Arctic
1071 Canada. *J. Paleolimnol.*, 1-15.

1072 Tipple, B.J., Berke, M.A., Hambach, B., Roden, J.S. and Ehleringer, J.R. (2015)
1073 Predicting leaf wax n -alkane $2H/1H$ ratios: controlled water source and humidity
1074 experiments with hydroponically grown trees confirm predictions of Craig-Gordon
1075 model. *Plant, Cell Environ.* 38, 1035-1047.

1076 Toolik Environmental Data Center Team (2016) Plant phenological monitoring
1077 program at Toolik, Alaska. Toolik Field Station, Institute of Arctic Biology, University
1078 of Alaska Fairbanks.

1079 Vachon, R., Welker, J., White, J. and Vaughn, B. (2010) Monthly precipitation
1080 isoscapes ($\delta^{18}O$) of the United States: Connections with surface temperatures,
1081 moisture source conditions, and air mass trajectories. *Journal of Geophysical*
1082 *Research: Atmospheres* 115.

1083 Walker, D. and Walker, M. (1996) Terrain and vegetation of the Innvait Creek
1084 watershed, Landscape Function and Disturbance in Arctic Tundra. Springer, pp. 73-
1085 108.

1086 Walker, D.A. and Maier, H.A. (2008) Vegetation in the vicinity of the Toolik Field
1087 Station, Alaska. University of Alaska. Institute of Arctic Biology.

1088 Walker, M.D., Walker, D.A. and Auerbach, N.A. (1994) Plant communities of a
1089 tussock tundra landscape in the Brooks Range Foothills, Alaska. *Journal of*
1090 *Vegetation Science* 5, 843-866.

1091 Ward, C.P. and Cory, R.M. (2015) Chemical composition of dissolved organic matter
1092 draining permafrost soils. *Geochim. Cosmochim. Acta* 167, 63-79.

1093 Welker, J. (2000) Isotopic ($\delta^{18}\text{O}$) characteristics of weekly precipitation collected
1094 across the USA: an initial analysis with application to water source studies.
1095 *Hydrological Processes* 14, 1449-1464.

1096 Welker, J.M. (2012) ENSO effects on $\delta^{18}\text{O}$, $\delta^2\text{H}$ and d - excess values in
1097 precipitation across the US using a high - density, long - term network (USNIP).
1098 *Rapid Commun. Mass Spectrom.* 26, 1893-1898.

1099 Welker, J.M., Rayback, S. and Henry, G.H. (2005) Arctic and North Atlantic Oscillation
1100 phase changes are recorded in the isotopes ($\delta^{18}\text{O}$ and $\delta^{13}\text{C}$) of *Cassiope tetragona*
1101 plants. *Global Change Biol.* 11, 997-1002.

1102 White, J.W., Cook, E.R. and Lawrence, J.R. (1985) The DH ratios of sap in trees:
1103 Implications for water sources and tree ring DH ratios. *Geochim. Cosmochim. Acta*
1104 49, 237-246.

1105 Wilkie, K., Chaplignin, B., Meyer, H., Burns, S., Petsch, S. and Brigham-Grette, J. (2012)
1106 Modern isotope hydrology and controls on δD of plant leaf waxes at Lake
1107 El'gygytyn, NE Russia. *Climate of the Past Discussions* 8, 3719-3764.

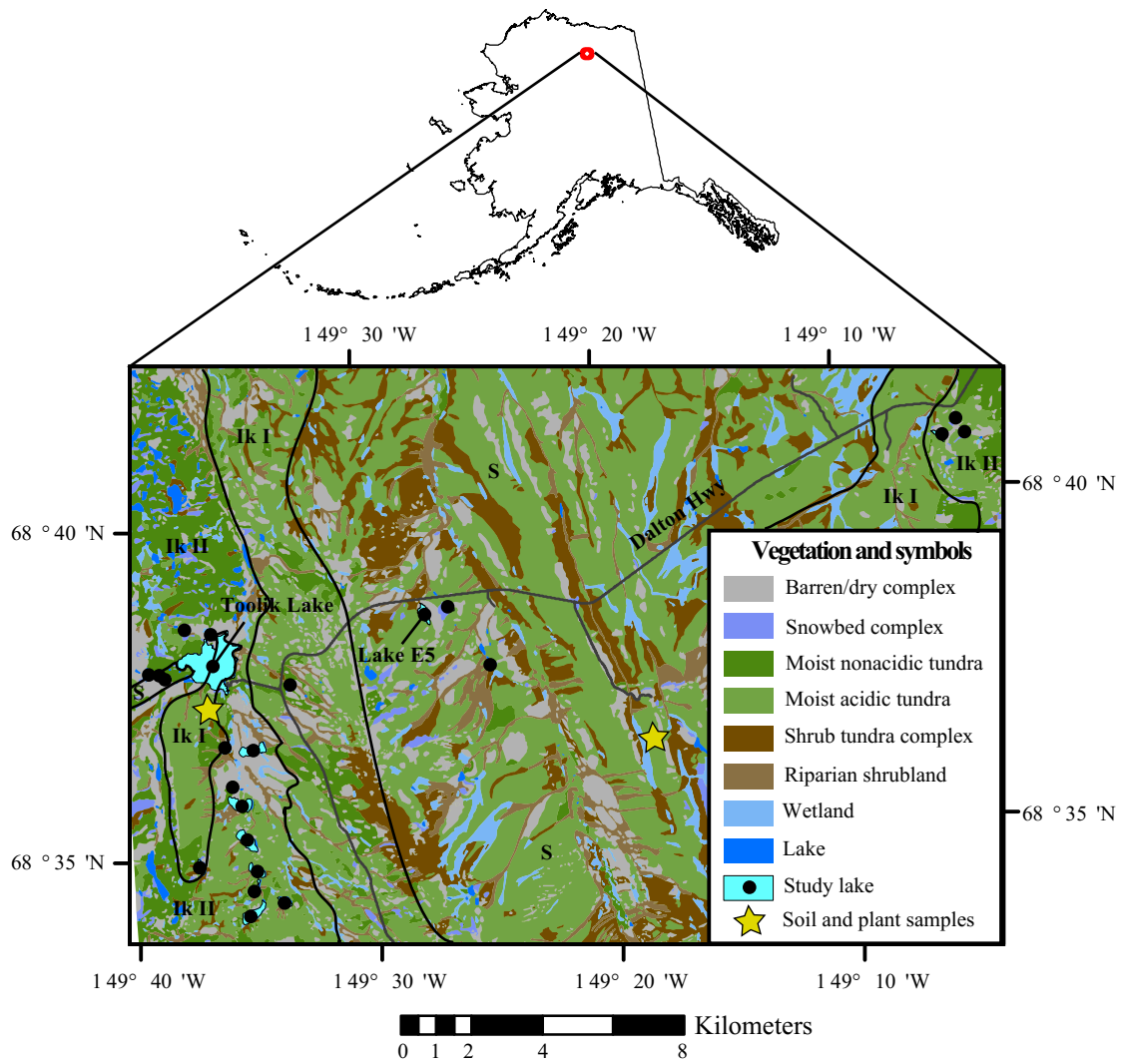
1108 Woo, M.-k. (2012) *Permafrost hydrology*. Springer Science & Business Media.

1109 Yang, H. and Huang, Y. (2003) Preservation of lipid hydrogen isotope ratios in
1110 Miocene lacustrine sediments and plant fossils at Clarkia, northern Idaho, USA. *Org.*
1111 *Geochem.* 34, 413-423.

1112 Yang, H., Liu, W., Leng, Q., Hren, M.T. and Pagani, M. (2011) Variation in n-alkane δD
1113 values from terrestrial plants at high latitude: Implications for paleoclimate
1114 reconstruction. *Org. Geochem.* 42, 283-288.

1115 Yang, H., Pagani, M., Briggs, D.E., Equiza, M., Jagels, R., Leng, Q. and LePage, B.A.
1116 (2009) Carbon and hydrogen isotope fractionation under continuous light:
1117 implications for paleoenvironmental interpretations of the High Arctic during
1118 Paleogene warming. *Oecologia* 160, 461-470.

1119 Young, J., Olga, K. and Welker, J.M. (In press) Thawing seasonal ground ice: an
1120 important water source for boreal forest plants in interior Alaska. *Ecohydrology*.
1121



1122

1123 Figure 1: Map of study lakes (black dots) and plant sampling locations (yellow stars).

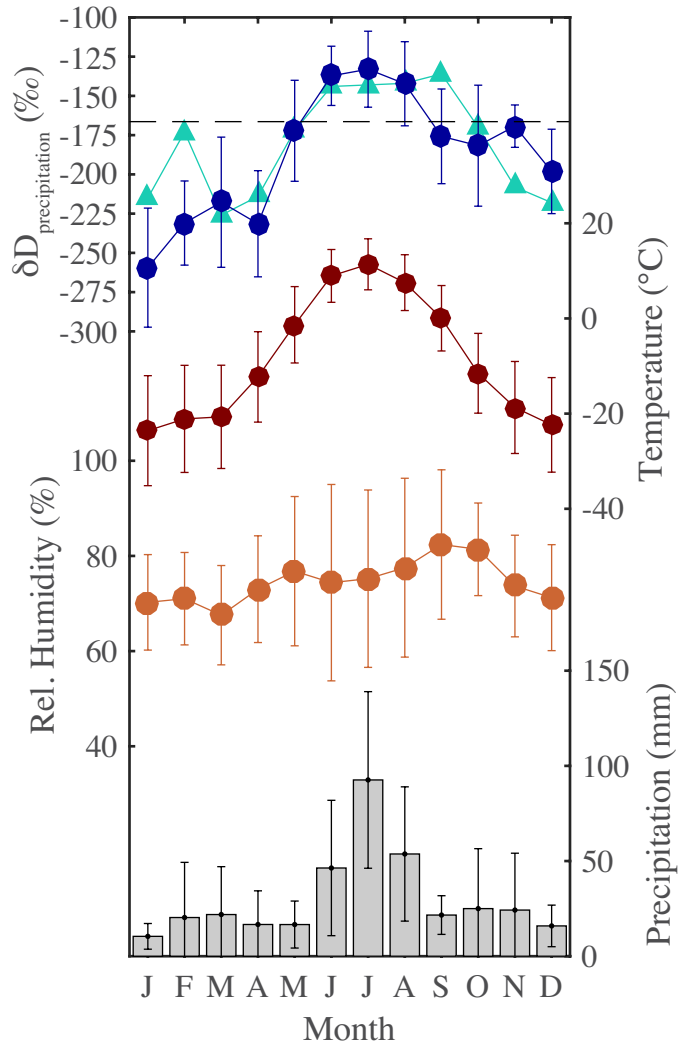
1124 The basemap shows the diversity of plant communities in the study area and a

1125 generalization of the glacial ages referenced in the text (<http://www.arcticatlas.org/>).

1126 Sediment traps were deployed in Lake E5 and Toolik Lake, as labelled on the map.

1127

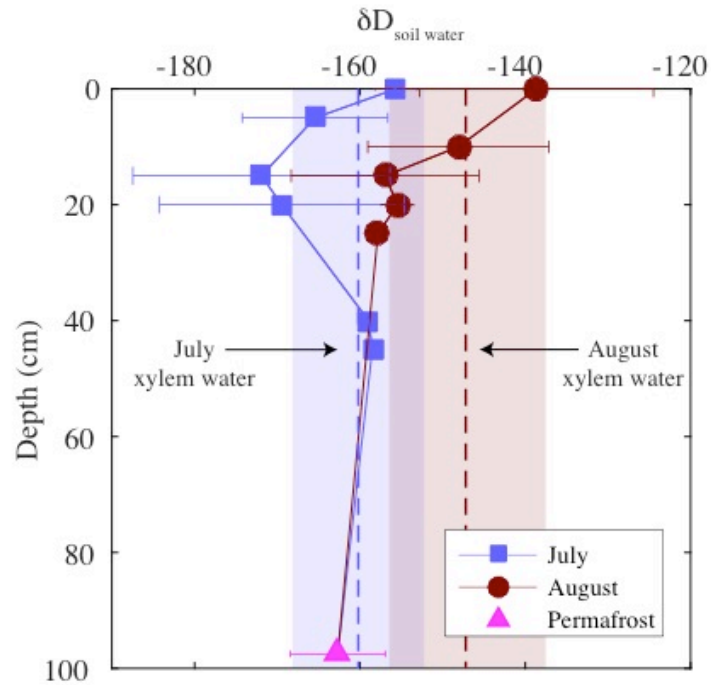
1128



1129

1130 Figure 2: Climatology and $\delta D_{\text{precipitation}}$ at Toolik Lake including monthly precipitation
1131 isotopes (blue – precipitation event measurements; green – OIPC estimate; the horizontal
1132 dashed line is the weighted mean annual $\delta D_{\text{precipitation}}$ value of -166 ‰), air temperature
1133 (red), relative humidity (orange), and precipitation (gray bars) (source: Toolik
1134 Environmental Data Center; accessed Nov. 2015).

1135



1136

1137 Figure 3. $\delta D_{\text{soil water}}$ profiles from July and August. The deep permafrost was sampled in

1138 July and is assumed to be constant throughout the year. Error bars are 1σ standard

1139 deviation from 1-6 replicate field samples; no error bar indicates $n=1$. Dashed vertical

1140 lines are δD_{xylem} from each sampling month (*E. vaginatum* and *B. nana* combined) and

1141 the shaded envelopes are 1σ standard deviation of xylem measurements based on

1142 multiple plants ($n=9$ for July, $n=13$ for August).

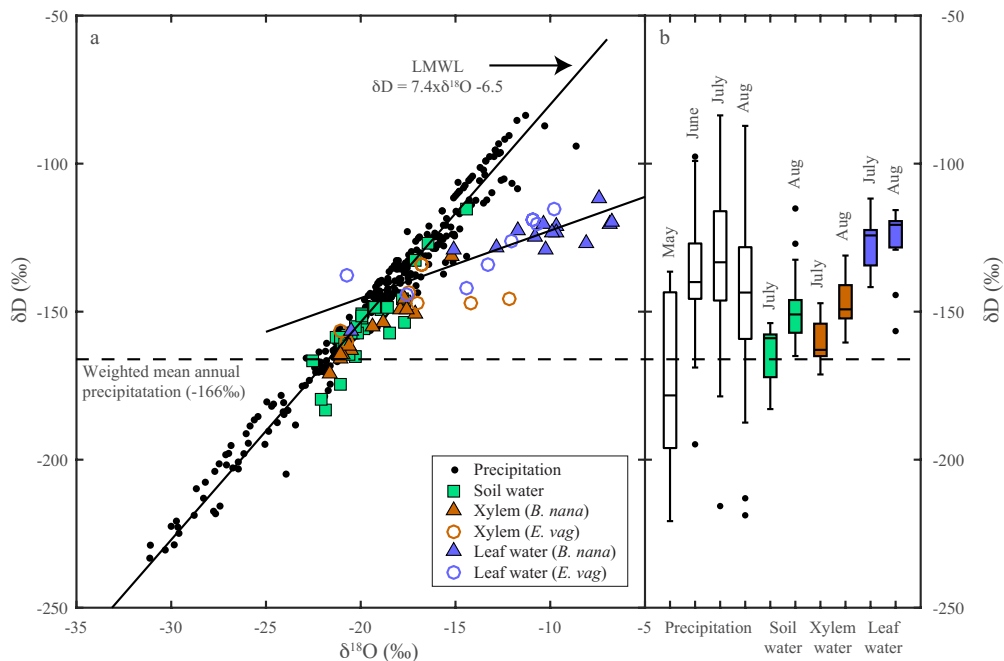
1143

1144

1145

1146

1147



1148

1149 Figure 4: Panel a: The relationship between δD and $\delta^{18}O$ at Toolik Lake for precipitation
 1150 (black points), soil water (green squares), plant xylem water of *B. nana* (orange triangles)
 1151 and *E. vaginatum* (orange circles), and leaf water of *B. nana* (blue triangles) and *E.*
 1152 *vaginatum* (blue circles). Nine precipitation isotope measurements were more depleted
 1153 than shown in the figure, reaching δD values as low as -316 ‰, but are omitted for clarity.
 1154 These lower values do not diverge systematically from the LMWL. The second
 1155 regression line goes through leaf water measurements and illustrates evaporative
 1156 enrichment in the leaves. Panel b: Summary figure of monthly $\delta D_{\text{precipitation}}$, δD_{soil} ,
 1157 δD_{xylem} , and δD_{leaf} . Xylem and leaf water plots combine data from both study species.
 1158 Boxes represent median, 25th and 75th percentiles, and whiskers extend to most extreme
 1159 non-outliers.

1160

1161

1162 Figure 5: Hydrogen isotope ratios of plant water and leaf waxes, and the net

1163 apparent fractionation between xylem water and leaf waxes for *Betula nana* and

1164 *Eriophorum vaginatum* in July and August. δD_{wax} and ϵ_{app} values represent averages

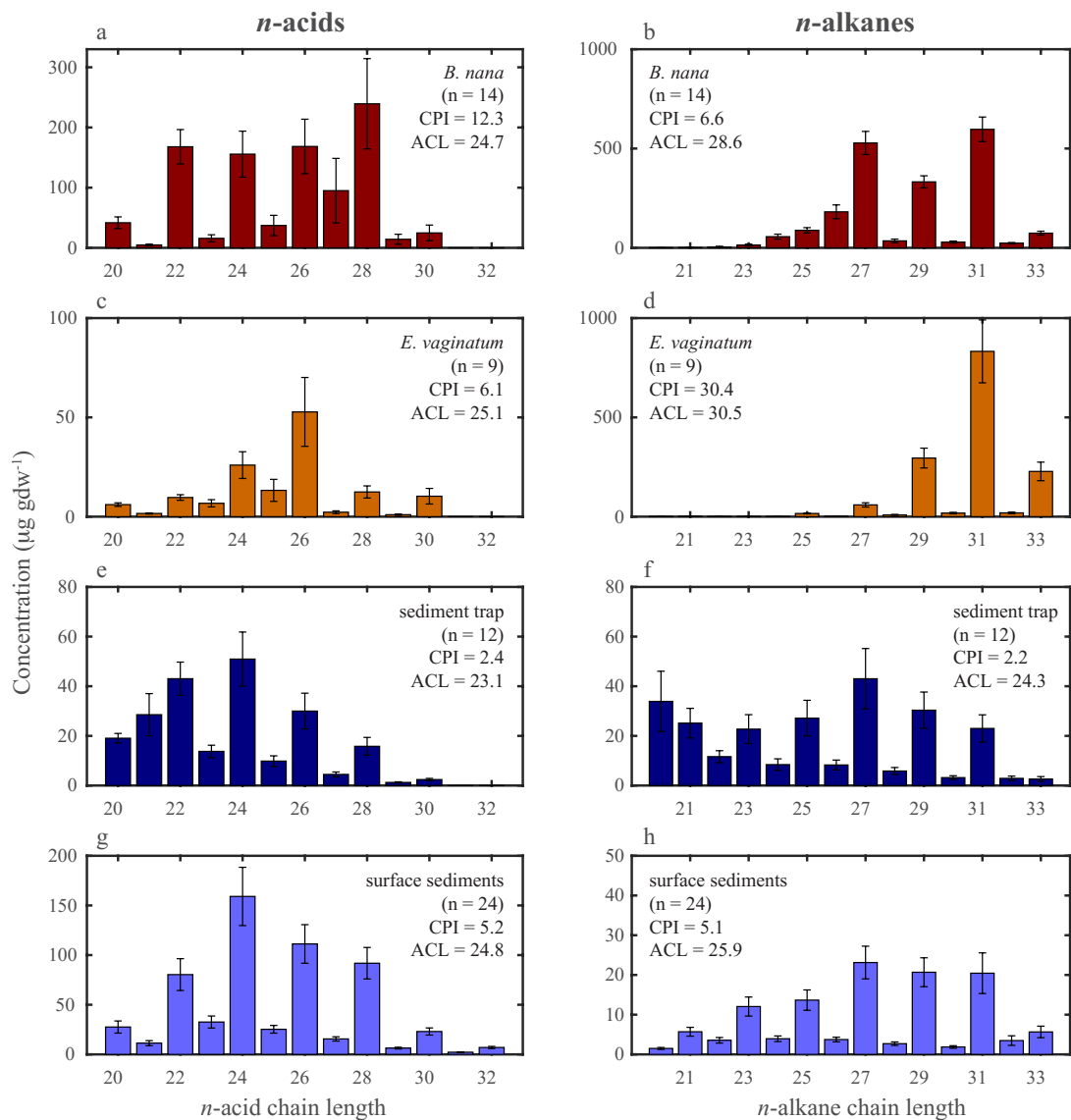
1165 of all measured lipid homologues. The month effect is not significant for values of

1166 ϵ_{app} , but is significant for xylem water in *Betula nana* and leaf water in *Eriophorum*

1167 *vaginatum*.

1168

1169



1170

1171 Figure 6: Concentration of long chain *n*-acids (C₂₀-C₃₂) and *n*-alkanes (C₂₀-C₃₃) in live

1172 specimens of *Betula nana* (panels a and b), *Eriophorum vaginatum* (panels c and d),

1173 sediment trap samples in Lake E5 (panels e and f), and surface sediments from lakes

1174 around Toolik Field Station (panels g and h). For plant samples, concentrations are given

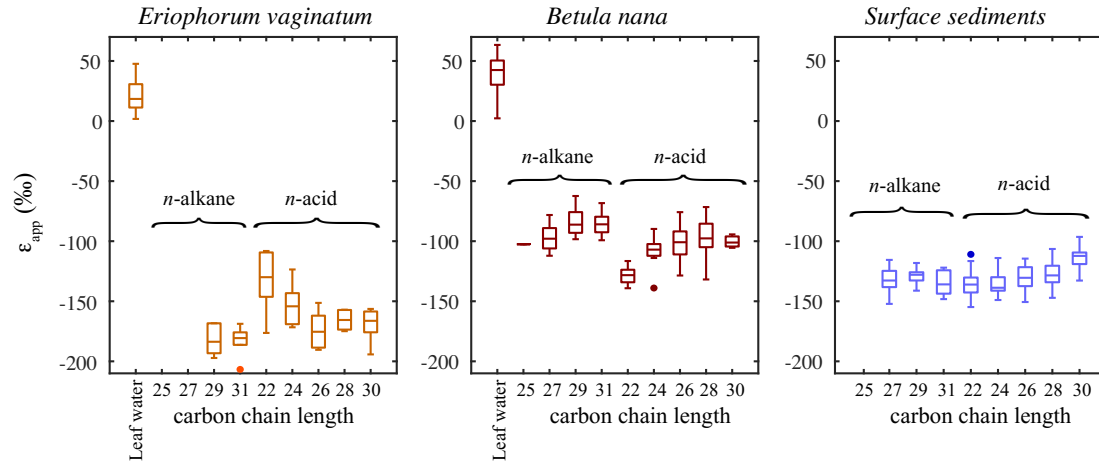
1175 relative to grams of dry leaf material, and for sediments it is relative to grams of dry

1176 sediment. Error bars represent standard error of the mean, while the n represents the total

1177 number of vegetation, sediment trap, and surface sediment samples.

1178

1179

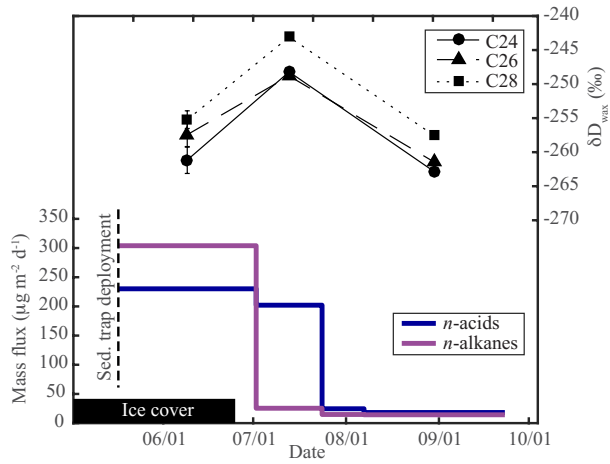


1180

1181 Figure 7: Net apparent D/H fractionation (ϵ_{app}) for a) *Eriophorum vaginatum* (C_3
1182 monocot; n = 9), b) *Betula nana* (C_3 shrub; n = 14), and c) lake surface sediments (n =
1183 24). For plant samples, fractionation is calculated relative to paired xylem water
1184 measurements, while for surface sediments, source water is set to the average of all
1185 xylem water measurements (-153‰). Boxes represent median, 25th and 75th percentiles,
1186 and whiskers extend to most extreme non-outliers.

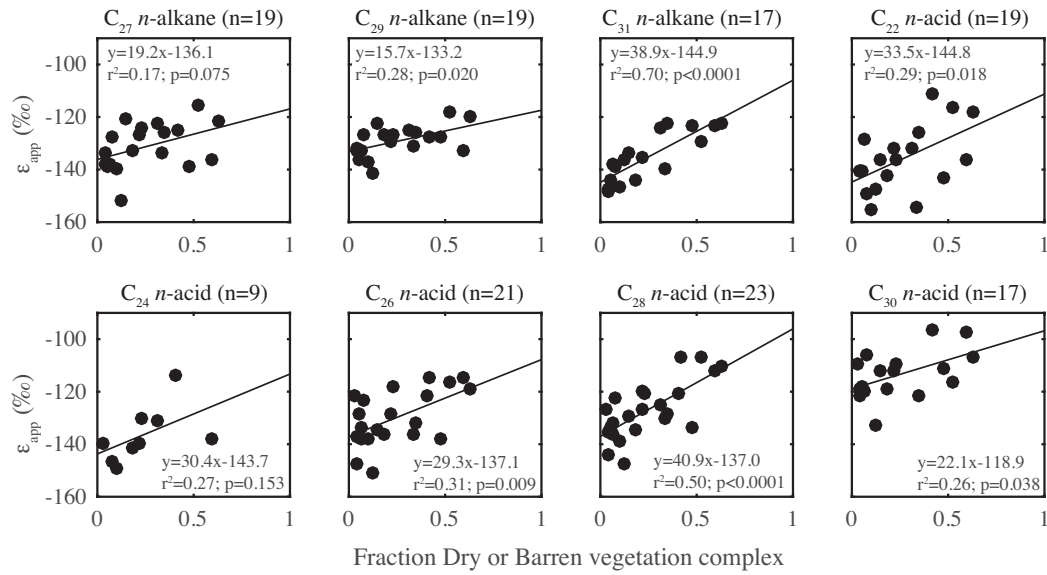
1187

1188



1189

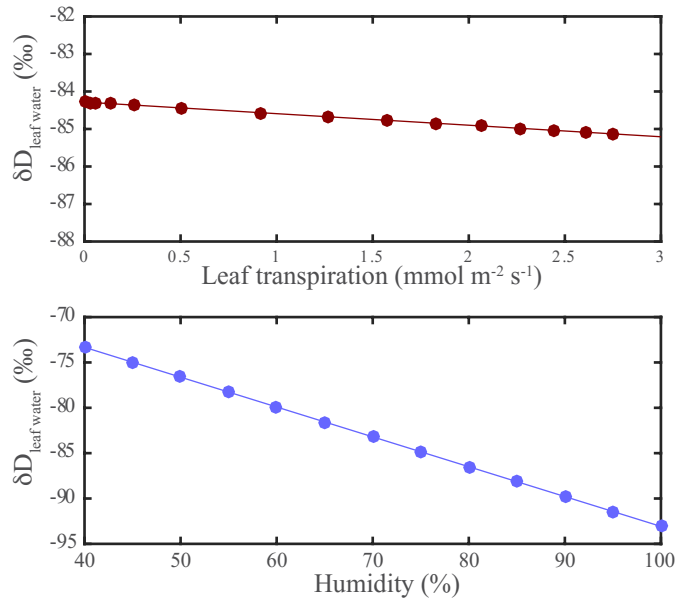
1190 Figure 8: *n*-acid and *n*-alkane fluxes and δD_{wax} , measured in sediment traps deployed in
1191 Lake E5 in 2014. Each point represents an average of 14-46 days of sediment collection.
1192 D/H ratios were measured on *n*-acids only, and are not available for the third collection
1193 because of insufficient sample mass. δD_{wax} error bars are standard deviation of 3
1194 sediment traps, but traps were composited prior to analysis for the later sampling dates.
1195



1196

1197 Figure 9: The relationship between surface sediment ϵ_{app} and the relative area of each
 1198 watershed comprised of dry or barren tundra (Alaska Geobotany Center,
 1199 <http://www.arcticatlas.org/>). Dry and barren tundra are dominated by shrubs and forbs
 1200 and have shallow organic soil layers (Walker et al., 1994). Fractionation factors are
 1201 calculated using a source water isotopic composition of -153‰, the average of all xylem
 1202 water measurements.

1203



1204

1205 Figure 10. Modeled leaf water isotopes under varying a) transpiration and b) humidity
 1206 conditions. The model used in this sensitivity analysis was developed by Tipple et al.
 1207 (2015) and uses JJA meteorological inputs from Toolik Lake Field Station (Toolik
 1208 Environmental Data Center Team, 2016), an initial source water isotope value of -153‰
 1209 (this study), and atmospheric vapor δD measured at Toolik Lake (Klein et al., 2015).

1210

1211

1212

1213

	Xylem water	<i>n</i> -acids					<i>n</i> -alkanes				
		C ₂₂	C ₂₄	C ₂₆	C ₂₈	C ₃₀	C ₂₅	C ₂₇	C ₂₉	C ₃₁	
<i>B. nana</i>											
δD (1σ)	6 Aug 2013 n=1	-131 (-)									
	12 July 2014 n=7	-165 (3)	-252 (-)	-243 (-)	-246 (-)			-245 (-)	-228 (-)	-216 (-)	
	7/8 Aug 2014 n=6	-152 (5)	-271 (7)	-252 (8)	-242 (5)	-238 (7)	-252 (3)		-239 (6)	-227 (7)	-232 (7)
	Average n=14	-156 (11)	-263 (6)	-245 (3)	-240 (6)	-237 (7)	-235 (8)	-243 (9)	-238 (5)	-228 (4)	-229 (5)
ε _{app} (1σ)	6 Aug 2013		-267 (7)	-248 (7)	-241 (5)	-238 (7)	-244 (11)	-243 (7)	-237 (6)	-227 (6)	-231 (6)
	17 July 2014		-139 (-)	-129 (-)	-132 (-)			-130 (-)	-112 (-)	-98 (-)	
	7/8 Aug 2014		-123 (6)	-100 (6)	-90 (9)	-85 (10)	-101 (-)		-87 (6)	-72 (8)	-78 (8)
	Average		-131 (6)	-109 (4)	-104 (7)	-100 (9)	-95 (1)	-104 (3)	-101 (4)	-89 (4)	-90 (4)
			-127 (7)	-108 (12)	-100 (13)	-96 (16)	-97 (4)	-113 (15)	-96 (10)	-82 (12)	-84 (9)
<i>E. vaginatum</i>											
δD (1σ)	6 Aug 2013 n=2	-134 (-)									
	12 July 2014 n=3	-150 (5)	-282 (1)	-298 (1)	-285 (1)						
	7/8 Aug 2014 n=4	-150 (8)	-248 (-)	-243 (25)	-259 (35)	-272 (24)	-295 (7)			-296 (2)	-303 (6)
	Average n=9	-145 (9)	-267 (20)	-278 (6)	-290 (4)	-283 (4)	-295 (14)			-308 (6)	-309 (9)
ε _{app} (1σ)	6 Aug 2013		-266 (20)	-272 (21)	-282 (27)	-278 (13)	-296 (12)			-303 (8)	-308 (8)
	17 July 2014		-171 (1)	-189 (2)	-174 (1)						
	7/8 Aug 2014		-108 (-)	-108 (22)	-127 (34)	-142 (21)	-170 (15)			-171 (3)	-180 (11)
	Average		-136 (28)	-150 (9)	-170 (7)	-161 (6)	-170 (13)			-189 (5)	-187 (10)
			-136 (28)	-148 (27)	-164 (36)	-160 (19)	-172 (12)			-183 (9)	-186 (8)

1214

1215 Table 1: The average δD_{wax} (‰) and net apparent fractionation (‰) of leaf waxes

1216 on living plants from all sites for each sampling date. Standard deviations in

1217 parentheses reflect variance between field samples, and n is the number of samples

1218 collected with each effort. Fractionation is calculated using paired xylem water

1219 measurements leaf wax measurements for each sample. Dashes mean not available.

1220

Lake Name	Lat.	Long.	Glacial Surface	Mean Depth (m)	Watershed area (ha)	Barren	Vegetation types (fraction of watershed)						
							Dry tundra	Snowbed	Moist non-acidic tundra	Moist acidic tundra	Shrub tundra	Riparian shrubland	Wetland
UCL	68.629	-149.413	S	-	264	0.01	0.06	0	0.02	0.42	0.07	0.38	0.03
E5	68.643	-149.458	S	6.3	129	0	0.21	0	0	0.69	0.01	0	0
E6	68.644	-149.439	S	1.6	26	0	0.21	0.34	0	0.37	0	0	0
E1	68.626	-149.554	IK I	3.1	87	0.13	0.17	0.04	0.16	0.32	0	0.14	0
I6HW	68.581	-149.619	IK I	3.6	56	0	0.13	0.07	0.31	0.16	0.23	0	0.01
Fog1	68.684	-149.079	IK II	8.4	22	0	0.06	0.07	0	0.75	0	0	0
Fog2	68.679	-149.089	IK II	7.8	37	0	0.27	0	0	0.58	0	0	0
Fog4	68.680	-149.072	IK II	2.1	55	0	0.23	0.08	0.02	0.59	0	0	0
Galbraith	68.460	-149.420	IK II	4.2	-	-	-	-	-	-	-	-	-
I1	68.569	-149.588	IK II	3.9	133	0	0.06	0	0.16	0.53	0.04	0.01	0.03
I2	68.571	-149.566	IK II	7.2	97	0	0.03	0	0.06	0.77	0	0.06	0
I3	68.575	-149.581	IK II	1.8	343	0	0.04	0	0.11	0.65	0.04	0.04	0.02
I4	68.580	-149.583	IK II	3.0	421	0	0.04	0	0.10	0.66	0.04	0.05	0.02
I5	68.587	-149.590	IK II	3.9	597	0	0.05	0	0.07	0.69	0.03	0.04	0.01
I6	68.597	-149.593	IK II	5.7	924	0	0.06	0.01	0.11	0.63	0.04	0.05	0.01
I7	68.601	-149.593	IK II	3.7	965	0	0.08	0	0.11	0.60	0.04	0.05	0.01
I8	68.610	-149.582	IK II	2.7	2970	0.03	0.12	0.03	0.12	0.45	0.12	0.09	0.03
Iswamp	68.611	-149.597	IK II	2.3	1227	0	0.11	0	0.12	0.57	0.03	0.07	0.02
N1	68.640	-149.604	IK II	4.8	32	0	0.53	0	0.22	0.05	0	0	0.04
N2	68.641	-149.622	IK II	5.0	21	0	0.28	0.20	0.07	0.31	0	0.07	0
S11	68.631	-149.648	IK II	3.3	24	0	0.36	0.03	0	0.54	0	0.04	0
S6	68.630	-149.639	IK-mix	3.0	796	0.02	0.29	0.08	0.35	0.14	0.04	0.03	0
S7	68.630	-149.643	IK-mix	0.8	40	0	0.44	0.1	0.13	0.33	0	0.03	0
TLK	68.632	-149.602	IK-mix	7.4	6486	0.02	0.16	0.2	0.15	0.42	0.07	0.08	0.02

1221 Table 2: Location, depths, and watershed characteristics of the 24 lakes from which
1222 we sampled surface sediment. S: Sagavanirktok (>125 ka), IK I: Itkillik I (~60 ka), IK
1223 II: Itkillik II (25-11.5 ka), IK-mix: mix of IK I and IK II. The sum of watershed cover
1224 classes are less than one because not shown is the area covered by lakes.

1225

Lake Name	Lat.	Long.	<i>n</i> -acids					<i>n</i> -alkanes		
			C ₂₂	C ₂₄	C ₂₆	C ₂₈	C ₃₀	C ₂₇	C ₂₉	C ₃₁
UCL	68.629	-149.413	-	-	-270	-265	-	-	-	-
E5	68.643	-149.458	-268	-263	-253	-255	-246	-258	-261	-
E6	68.644	-149.439	-268	-270	-250	-248	-235	-269	-266	-258
E1	68.626	-149.554	-260	-	-265	-262	-256	-259	-259	-257
I6HW	68.581	-149.619	-265	-271	-262	-260	-248	-260	-263	-268
FOG1	68.684	-149.079	-268	-	-267	-263	-248	-255	-257	-267
FOG2	68.679	-149.089	-265	-264	-	-259	-	-257	-259	-258
FOG4	68.680	-149.072	-284	-	-269	-263	-	-266	-264	-271
GALBRAITH	68.460	-149.420	-267	-262	-260	-262	-246	-	-	-
I1	68.569	-149.588	-279	-277	-257	-256	-243	-261	-260	-271
I2	68.571	-149.566	-	-271	-256	-260	-246	-	-	-
I3	68.575	-149.581	-272	-	-278	-275	-256	-270	-265	-278
I4	68.580	-149.583	-272	-	-269	-268	-254	-266	-264	-278
I5	68.587	-149.590	-272	-	-262	-266	-253	-271	-268	-275
I6	68.597	-149.593	-262	-	-266	-268	-255	-270	-265	-270
I7	68.601	-149.593	-284	-279	-270	-270	-	-271	-269	-277
I8	68.610	-149.582	-274	-273	-268	-267	-254	-265	-260	-275
ISWAMP	68.611	-149.597	-278	-	-281	-278	-265	-282	-273	-268
N1	68.640	-149.604	-253	-	-254	-247	-243	-256	-255	-256
N2	68.641	-149.622	-252	-	-251	-244	-251	-251	-253	-262
S11	68.631	-149.648	-	-250	-256	-255	-	-	-	-
S6	68.630	-149.639	-247	-	-250	-243	-235	-259	-261	-
S7	68.630	-149.643	-274	-	-269	-267	-247	-270	-261	-257
TLK	68.632	-149.602	-	-	-	-254	-	-	-	-
Average δD_{wax} (1σ)			-268 (10)	-268 (9)	-263 (9)	-261 (9)	-249 (8)		-264 (8)	-262 (5)
Average ϵ_{app} (1σ)			-136 (12)	-136 (10)	-130 (10)	-127 (11)	-113 (9)		-131 (9)	-129 (6)

1227 Table 3: δD_{wax} and apparent fractionation (‰) of lake surface sediments.

1228 Fractionation is calculated using a source water value of -153‰ based on xylem

1229 water observations for the two plant species. Dashes mean not measured.

1230